

Integrated Experimental and Numerical Research on the Aerodynamics of Unsteady Moving Aircraft

1. Dr.-Ing. Andreas Bergmann, German-Dutch Wind Tunnels (DNW)
2. Dipl.-Ing. Andreas Hübner, German Aerospace Center (DLR)

1. DNW
German-Dutch Wind Tunnels
Lilienthalplatz 7
38108 Braunschweig
Germany
andreas.bergmann@dnw.aero

2. DLR
German Aerospace Center
Lilienthalplatz 7
38108 Braunschweig
Germany
andreas.huebner@dlr.de

Abstract

For the experimental determination of the dynamic wind tunnel data a new combined motion test capability was developed at the German-Dutch Wind Tunnels DNW for their 3m Low Speed Wind Tunnel NWB in Braunschweig, Germany, using a unique six degree-of-freedom test rig called 'Model Positioning Mechanism' (MPM) as an improved successor to the older systems. With that cutting-edge device several transport aircraft configurations including a blended wing body configuration were tested in different modes of oscillatory motions roll, pitch and yaw as well as delta wing geometries like X-31 equipped with remote controlled rudders and flaps to be able to simulate realistic flight maneuvers, e.g. a dutch-roll.

This paper describes the motivation behind these tests and the test setup and in addition gives a short introduction into time accurate maneuver testing capabilities incorporating models with remote controlled control surfaces. Furthermore, the adaptation of numerical methods for the prediction of dynamic derivatives is described and some examples with the DLR-F12 configuration will be given. The calculations are based on RANS-solution using the finite volume parallel solution algorithm with an unstructured discretization concept (DLR TAU-code).

Key words: unsteady aerodynamics, dynamic wind tunnel experiments, maneuvering aircraft, dynamic derivatives, Panel/EULER/RANS-solution, model positioning mechanism, movement device

Report Documentation Page				Form Approved OMB No. 0704-0188	
Public reporting burden for the collection of information is estimated to average 1 hour per response, including the time for reviewing instructions, searching existing data sources, gathering and maintaining the data needed, and completing and reviewing the collection of information. Send comments regarding this burden estimate or any other aspect of this collection of information, including suggestions for reducing this burden, to Washington Headquarters Services, Directorate for Information Operations and Reports, 1215 Jefferson Davis Highway, Suite 1204, Arlington VA 22202-4302. Respondents should be aware that notwithstanding any other provision of law, no person shall be subject to a penalty for failing to comply with a collection of information if it does not display a currently valid OMB control number.					
1. REPORT DATE JUN 2007		2. REPORT TYPE N/A		3. DATES COVERED -	
4. TITLE AND SUBTITLE Integrated Experimental and Numerical Research on the Aerodynamics of Unsteady Moving Aircraft				5a. CONTRACT NUMBER	
				5b. GRANT NUMBER	
				5c. PROGRAM ELEMENT NUMBER	
6. AUTHOR(S)				5d. PROJECT NUMBER	
				5e. TASK NUMBER	
				5f. WORK UNIT NUMBER	
7. PERFORMING ORGANIZATION NAME(S) AND ADDRESS(ES) DNW German-Dutch Wind Tunnels Lilienthalplatz 7 38108 Braunschweig Germany				8. PERFORMING ORGANIZATION REPORT NUMBER	
9. SPONSORING/MONITORING AGENCY NAME(S) AND ADDRESS(ES)				10. SPONSOR/MONITOR'S ACRONYM(S)	
				11. SPONSOR/MONITOR'S REPORT NUMBER(S)	
12. DISTRIBUTION/AVAILABILITY STATEMENT Approved for public release, distribution unlimited					
13. SUPPLEMENTARY NOTES Third International Symposium on Integrating CFD and Experiments in Aerodynamics, June 2007, The original document contains color images.					
14. ABSTRACT					
15. SUBJECT TERMS					
16. SECURITY CLASSIFICATION OF:			17. LIMITATION OF ABSTRACT UU	18. NUMBER OF PAGES 50	19a. NAME OF RESPONSIBLE PERSON
a. REPORT unclassified	b. ABSTRACT unclassified	c. THIS PAGE unclassified			

Overview, Current Situation and Motivation

During the expensive process of aircraft development it is highly desirable to obtain information about the future flight mechanics behavior of an aircraft already at a very early stage. The reliability of the predicted data is of eminent importance with regard to cost effectiveness within the design process. For the upcoming new airplane configurations (e.g. wide body, green aircraft, blended wing body) the approach up to now using semi-empirical methods as standard prediction tools is not as accurate as required. Hence the DLR Institute of Aerodynamics and Flow Technology in Braunschweig, Germany, started to develop a new method for the reliable determination of the dynamic derivatives to be able to describe the handling qualities sufficiently and to be able to predict the dynamic loads of a new aircraft fairly. Of particular importance for the success of that project was a distinct improvement of the state-of-the-art measuring techniques to experimentally determine the derivatives as it was felt to be mandatory to validate the numerical method with a reliable experimental database. But during the development phase it turned out that just with close interaction between CFD and wind tunnel test environment a proper progress could be achieved.

Dynamic wind tunnel testing has been performed since 30 years in the Low Speed Wind Tunnel DNW-NWB in Braunschweig. The two relevant model supports and the corresponding data acquisition equipment suitable for dynamic wind tunnel measurements will be described in some detail.

One model support is a classical Rolling and Spinning Derivative Support (RTD) which enables the model to perform a continuous rolling and spinning motion about the wind axis.

The other dynamic model support is the Model Positioning Mechanism (MPM) that complements the above mentioned RTD. The development and the performance of the MPM will be described as well as the instrumentation necessary for dynamic tests that includes the stereo pattern recognition technique with CMOS cameras. This system is used for determining the time-dependent model position and for measuring the appearing wing shape during a 3 Hz forced sinusoidal oscillation as well as during combined motions to simulate realistic flight maneuvers. The quality and performance of the dynamic instrumentation is of special importance as the quality of the results of dynamic measurements depends strongly upon the quality of the measurement of the model's instantaneous position with respect to the simultaneousness of the position signal and balance and pressure signals. This especially holds true when separate measurement systems are used for force / pressure and position measurement as is the case at DNW-NWB.

A first general survey about the determination of dynamic stability derivatives, necessary for the identification of the dynamic characteristic of aircrafts and for the calculation of the structural loads on individual components, is given in [1] in which an article by K.J. Orlik-Rückemann, giving an overview about different techniques for the experimental determination of dynamic derivatives, can be found, see also [2]. Furthermore, in [3] the changing interest in the determination of dynamic derivatives regarding the requirements of increasing angles of attack during the seventies of the 20th century is described. At extreme flight attitudes and on slender configurations with non-linear aerodynamic characteristics, e.g. by means of high angles of attack, strakes, transonic effects, it is up to nowadays very difficult to predict the airflow and therewith the aircraft's behavior correctly. This of course especially holds true in the seventies. Of particular importance is, at that time as today, the determination of confidence levels and standard deviations which have to be taken into account in the correlation between theory, wind tunnel test and flight test.

Aerodynamic tests on maneuvers with high amplitudes and high velocities of highly agile combat aircraft were of interest at that time and furthermore in the sixties and seventies the slender configurations like e.g. Space Shuttle, Sängers and Concorde were the motivation for very comprehensive activities to investigate the relevant flow regime. From this the demand for extensive dynamic wind tunnel tests in the western world can be derived, cp. thereto the aerodynamic flight mechanical Conference Proceedings, besides [1] also [4], [5]. The latter is in close association with [6] in which the rolling and spinning experiments are discussed in some detail. The essential conclusion here was that all achievements show good correlation as long as the airflow is clear without ambiguity. But if the flow is

able to reach different states under same constraints, however, the results rather depend on the wind tunnel in which the tests were performed. From this it was ever tried to define boundaries inside of which safe flow states exist and within an airplane control system can work reliably. But with the requirements for predictions of rapid high angle-of-attack maneuvers it was found out that more studies about rather complex and unorthodox configurations were necessary with extension of the speed range and with including data of time history effects, scale effects and aerodynamic interference effects. As the so far gained experimental data seemed to be insufficient to draw conclusions regarding these points a new AGARD activity was started in the nineties, see [7], which provides for the first time a comprehensive database for rotary and oscillatory characteristics of a generic WG16 fighter type model configuration over a large range of angles of attack as well as comprehensive results on surface pressures, forces and moments for validation of in this field so far not existing reliable numerical codes. More validation experiments on simple generic shapes designed to provide detailed measured data for the verification of results from CFD codes are given in [8]. Here the results for oscillating and transient movement patterns of complete configurations and for oscillating flaps can be found, including calculations of dynamic force and pressure measurements on an Oscillating 65° Delta Wing by DaimlerChrysler Aerospace as well as measurements by DLR at DNW-NWB. That can be seen as one of the first examples of a fruitful interaction between experimental and numerical work as the data evaluation could be well improved by the experience from the calculations, see also [9].

The determination of the dynamic derivatives in DNW-NWB in Braunschweig, Germany, started in the seventies with the Mobile Oscillatory Balance MOD, [8], [10], [11], and with the rolling and spinning device RTD, [7], [10], [11], with the configurations Alpha-Jet and MRCA Tornado being the most prominent test objects. This kind of testing has been resumed after two decades of decommission in collaboration with the Institute of Aerodynamics and Flow Technology of DLR within the German MEGAFLUG project. This project was started to improve the assessment of the aerodynamic properties of the planned Airbus Megaliner. In particular the contributions of the individual components of the airplane should be quantified more precisely compared to the industrial handbook methods so far commonly used, see [12]. The investigations proceeded with the development of a numerical prediction tool for aerospace applications. This method is described in [13] in some detail, where in a first step for more detailed understanding of the unsteady aerodynamic and flight mechanical behavior of an airplane schematic investigations on basic configurations with a NACA0012 airfoil have been used. In [14] more results from calculations of the dynamic derivatives of a modern transport aircraft configuration DLR-F12 are presented, compared with results from corresponding experiments in DNW-NWB. The focus here is not only put upon the evaluation of flight properties and to obtain data for the estimation of the dynamic structural loads on individual components but also on gaining a database for validation of newly developed CFD tools. A complex time accurate maneuver on a detailed X31-canard configuration with time accurate remote controlled rudders and flaps is described in [15]. This can be seen as a first step to provide a database for validation of recently developed multidisciplinary time accurate CFD-codes for calculating a free flying aeroelastic maneuvering combat aircraft. Here the computational aerodynamic, structural and flight mechanic codes are embedded into a simulation environment. Hence it is the goal for a proper validation to get nowadays corresponding results from wind tunnel tests, implying not only time accurate force measurements but also pressure distribution, model movement and determination of the corresponding change of the wing's twist and bending.

There is no denying that with the upcoming available calculation tools and with the ever advancing calculation power the recent trend of the development in aerodynamic research shows a fruitful interaction between CFD and experimental work that is not only much closer today than in the past but also very efficient and progressive. One of the major outcomes of this project is that only the combination of theory and experiment is sufficient to get proper insight into the flow physics and a better understanding of the relevant relating facts. It will be shown that just the interaction between CFD and wind tunnel has led to a proper aerodynamic investigation of the field of dynamic flight behavior, mandatory for the development of future prediction tools.

Facility

The DNW-NWB belongs to the foundation German-Dutch Wind Tunnels DNW. It is an atmospheric wind tunnel of closed-circuit type and has a test section size of $2.8 \cdot 3.25 \text{ m}^2$ with a maximum free stream velocity of about 85 m/s

(280 ft/s). It can be operated optionally with a closed, a slotted or an open test section. The DNW-NWB has recently been considerably upgraded regarding its control systems, measuring techniques and heat exchanger.

Rotary-Balance Apparatus

The rotary-balance test technique, developed to provide information on the effects of angular rates on the aerodynamic forces and moments on a flying aircraft, is described comprehensively in [6] and the corresponding RTD apparatus at DNW-NWB has remained unchanged since the first measurements in 1977. The model is fixed to a support system that can be rotated at constant rates about the free stream velocity vector of the wind tunnel. Thus the attitude of the model remains constant with respect to the airstream throughout a rotational cycle. The flow can be considered as steady-state. The forces and moments are determined by a six-component internal strain-gauge balance. It can be taken from Fig. 1 and 2 that the RTD can be operated both in the closed and in the open test section of the DNW-NWB. The apparatus is driven by a servo-controlled hydraulic motor. The rotation rate can be varied up to 300 rpm. While rotating the model its angle of attack can be changed over a range of 30° . By using existing different cranked stings the adjustable angle of attack constitutes from -30° to $+90^\circ$. The angle of sideslip can be changed between $\pm 90^\circ$ by adjusting the front part of the sting manually. The RTD can be operated in the rigging bay beneath the test section while another test is running. After completion of the model instrumentation and all relevant test preparations the RTD can be lifted by spindle drives from the rigging bay into the test section to continue with wind tunnel operation without time delay. For description of a typical test procedure and data reduction please refer to [6].

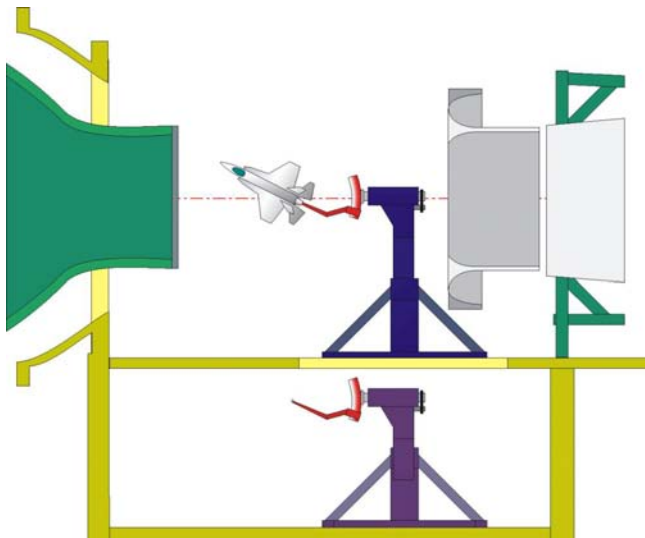


Figure 1. Rotary balance RTD of DNW-NWB – sketch.

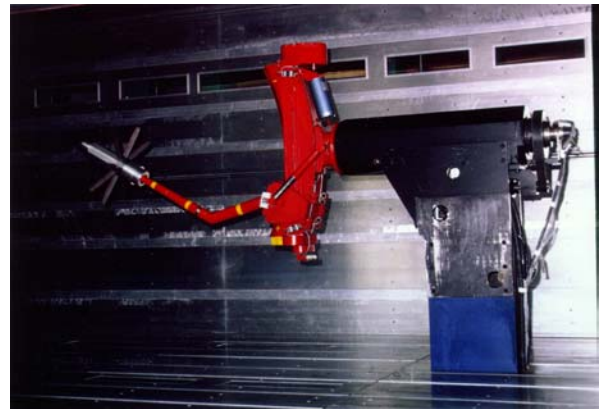


Figure 2. Photograph of RTD in the closed test section of DNW-NWB.

Oscillatory Motion Apparatus

As aforementioned, the classical so far known oscillatory balance of DNW-NWB (MOD), see Fig. 3, has been replaced since the end of the nineties successively, starting within the MEGAFLUG project, by improved elements.



Figure 3. The MOD test setup in the DNW-NWB with an A380 configuration.

In a first step a new support called the Oscillatory Model Support (OMS) of DNW-NWB was developed [16]. At serial kinematic structures, as depicted in Fig. 1 to 3, the number of DoF is achieved by serial arrangement of the corresponding number of linear and rotative axes. So the bottom-most axis of movement has to carry the weight of all those lying above it and this results in a contradiction between the requirement for high stiffness (high mass) and high dynamics (low mass). In addition to that all errors (thermal, geometric, caused by loads, ...) of movement of all axes are added. As parallel kinematics get rid of these problems it was decided to choose a kinematics of Hexapod type (Stewart platform) for the OMS. This motion apparatus excites the forced sinusoidal model oscillations in the modes pitch, roll, yaw, heave and lateral oscillation about arbitrary oscillation axes but usually oscillations are performed about model-fixed or wind-fixed oscillation axes.



Figure 4. The OMS test setup in the DNW-NWB with an A380 configuration.

Fig. 4 shows the model mounted on a belly sting which is fixed to the movable frame of a hydraulic platform having six degrees of freedom. The platform incorporates six hydraulic jacks. An additional hydraulic actuator which is located on the Stewart platform is used to excite the pitch and roll oscillation of the model (Fig. 5) via a suitable kinematics inside the model's fuselage that transforms the translatory motion of the additional actuator into the required rotatory motions. Larger amplitudes and higher oscillation frequencies are possible this way because it saves the Hexapod's upper frame from moving along a circular path with a radius of approximately 6 ft what doubtlessly is also possible but what creates large unfavorable inertia effects. For more information about the OMS and about the applied test procedures please refer to [12].

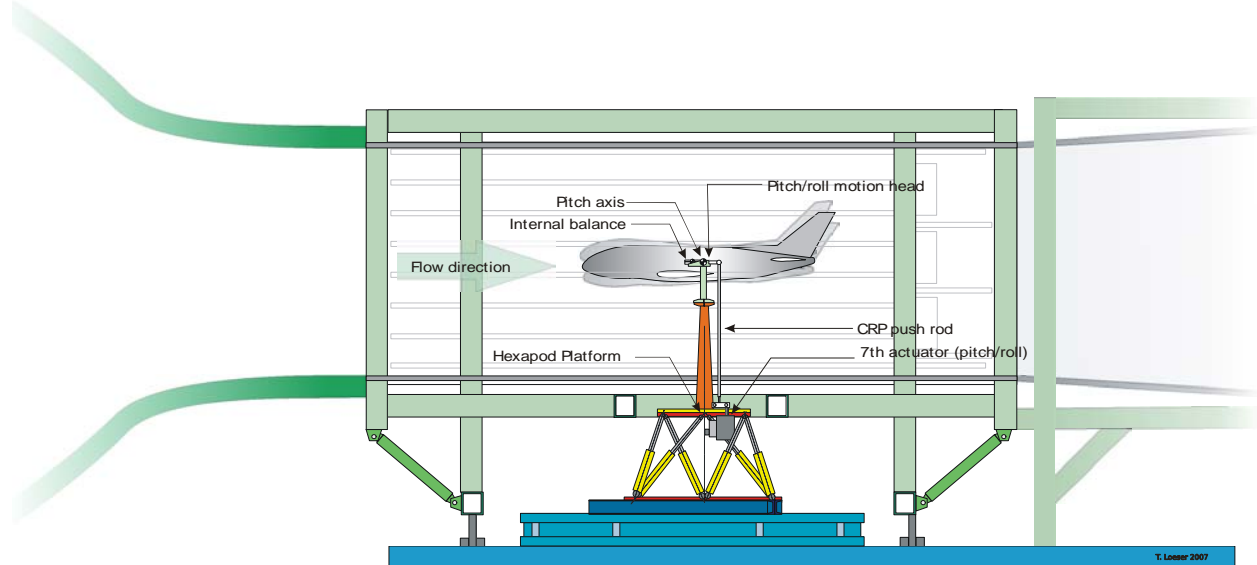


Figure 5. Schematic view of the OMS test setup.

The idea to use the Stewart platform and utilizing its variability as great advantage in a wind tunnel is not new. A first analysis for using a parallel kinematics as a test rig in a wind tunnel has been made in [17], but to the authors' knowledge this matter was not followed up as the inherent large number of singular positions (i.e. locations in the workspace at which the stiffness at the tool in definite directions disappears. In the vicinity to such singularities the stiffness is at least very low.) of the proposed kinematics restricted the available workspace. Besides that, the large number of joints were challenging for stiffness and precision.

Nevertheless, the selection of this kind of six degree-of-freedom dynamic test rig as parallel kinematics for the DNW-NWB gives several advantages compared to a conventional multi-axes test rig in serial arrangement:

- Higher dynamics despite identical input power because lower weights are being moved
- Higher accuracy because errors of single axes are not added
- Higher stiffness regarding the weight of the components because only forces in axial direction of the legs are acting

Of course, the inherent disadvantages are serious and might be the reason why this type of apparatus is not so commonly used as test rig in wind tunnel facilities. Beside the singularity problems the available working space is relatively small compared to the size of the machine. That means that enlarging the working space leads to an exceedingly large and heavy machine counteracting the advantage of a proper dynamic behavior.

To overcome these difficulties a new six degree-of-freedom model support called 'Model Positioning Mechanism' (MPM) was developed by DLR and DNW in 2004 as an improved successor to MOD and OMS.

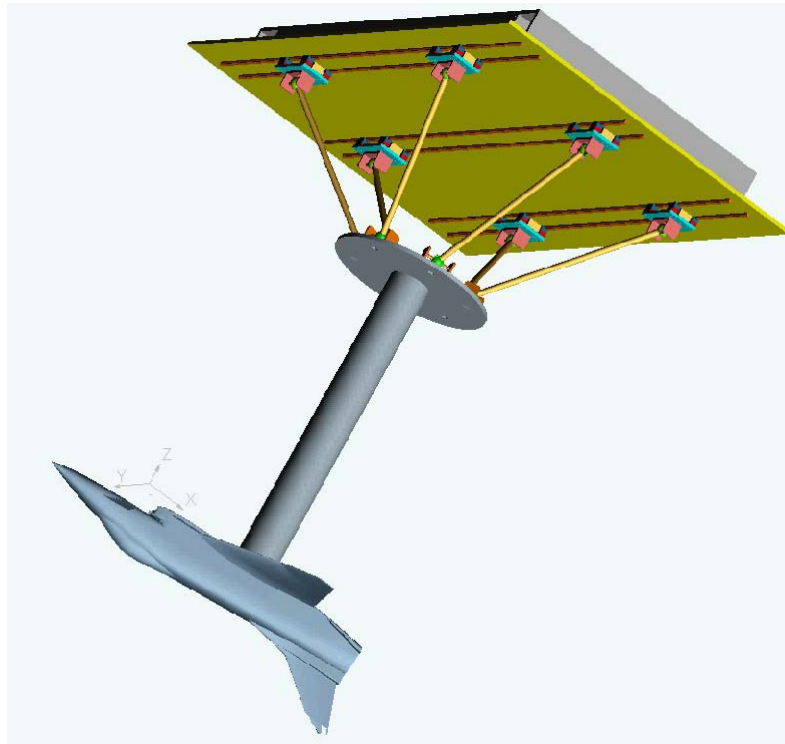


Figure 6. Principle of the MPM parallel kinematic machine.

This novel and so far unique MPM is also based on a parallel kinematic concept. The principle of the kinematic is depicted in Fig. 6. It is based on an idea of Wiegand [18], see also [19], from ETH Zurich with the intention to realize a parallel manipulator to be used as a high speed milling machine. It consists of a movable platform which is linked to the wind tunnel fixed base by six constant length legs – joined with the platform as well as with six carriages which can move along parallel guiding rails so that the position and orientation of the platform can be adjusted. The six carriages run independently from each other on each guiding rail, allowing a displacement within six degrees of freedom. The test rig can be used for oscillating the wind tunnel model about one body axis through a sinusoidal motion as well as for combined motions to simulate realistic flight maneuvers, e.g. a dutch-roll. It is located above the test section so that it can be used not only for dynamic measurements but also for ground effect simulation. The realized design as a result of an optimization against stiffness can be seen in Fig. 7. Because each guiding rail is shared by three carriages the design is simplified and has fewer components than previous versions [20]. The major characteristic of the MPM is its high dynamic capability combined with high and nearly constant stiffness over the whole workspace which spans 1100 mm in flow direction, 300 mm in lateral direction and 500 mm in heave direction, without singular positions. To avoid a conventional ballscrew drive with all its elasticity in the drive chain the axes are brought into motion by application of the linear direct drive technology. The accuracy of the system in pivoting angles is better than 0.005° . The first Eigenfrequency at the sting's end is above 20 Hz. The MPM can be operated in the open test section as well as in the closed one.

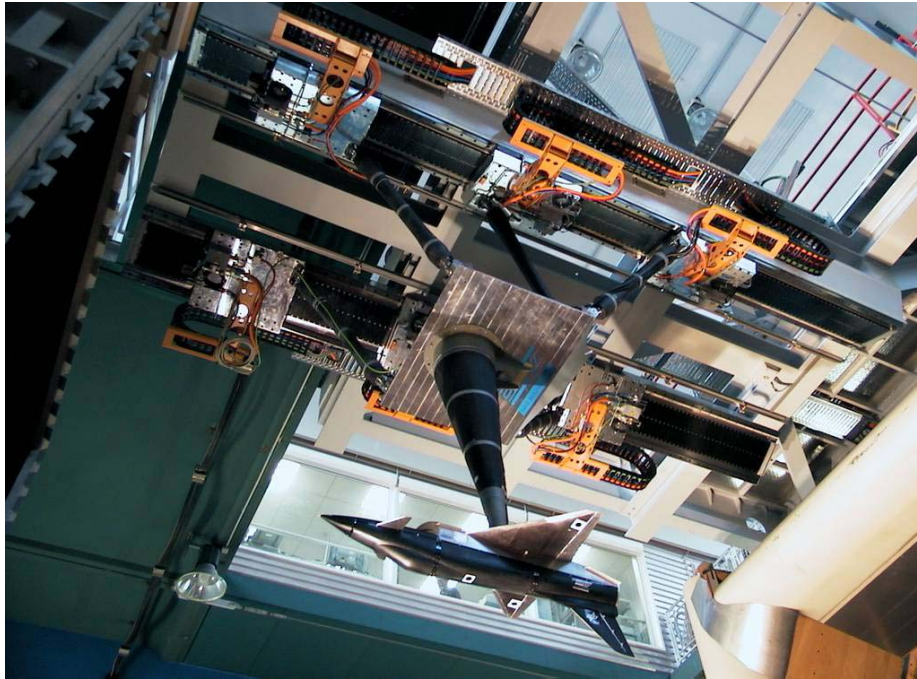


Figure 7. Realized MPM kinematic design in DNW-NWB with X-31.

Data Evaluation

For the evaluation of the derivatives it is assumed that the aerodynamic force and moments are linear functions of model position and angular speed or, in case of heave and lateral oscillation, to be linear functions of translatory speed and acceleration. For configurations on which vertical and/or separated flow cause non-linear characteristics more sophisticated mathematical models are required. Furthermore, the wind tunnel model is assumed to be ideally stiff. Because the wind-on balance signals contain both aerodynamic and inertial forces the latter have to be subtracted from the wind-on data. This is i.e. possible if model weight, center of gravity and moments of inertia are known. Another more practical solution is to determine the inertial forces by measuring the forces acting on an oscillating model in wind-off condition. For more details please refer to [12].

Measurement of Model Position

On the MOD the measurement of the unsteady model position was done by means of a strain gauge on a spring loaded lever located far away from the model below the test section floor. This system had the disadvantage of not recording deviations of the model position due to elasticity of the mechanical setup or due to play in the bearings between the strain gauge position and the model itself. A similar technique is the suitable application of an electric longimetry sensor in the vicinity of the moving frame of the OMS. From Fig. 8 it can be taken how the position of the model's fuselage interacts with the sensor to get information about the unsteady position of the model within one oscillation mode.

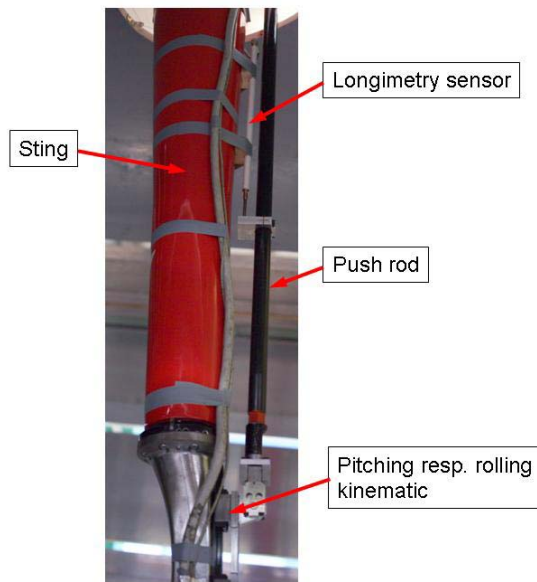


Figure 8. Application of the electric sensor for information of the model's attitude.

Another applied method is the use of an optical position measuring system. A high speed digital video camera from Pulnix Company, recording the position of distinct markers on the model, provides the values of translatory displacement and angular deflection in real time with a frequency up to 300 Hz at a resolution of 648 x 100 pixels. Image acquisition and real time processing are done with a dual P-III personal computer which is equipped with a Viper frame grabber card and a specifically adopted version of the PicColor software [21].

This method has the advantage of achieving the amplitudes of the model correctly but extraordinary diligence has to be taken on the triggering of the video camera as it is shown below that the phase relationship between the model position signals and the balance signals is of great importance for the accuracy of the derived dynamic derivative coefficients.

Fig. 9 shows the installation of the camera on the test section side wall protected against the flow to minimize vibrations and the installation of the mercury vapor lamp which is necessary to illuminate markers implemented on the model. Fig. 10 shows the markers on the fuselage, among holes and screw heads in their vicinity, which are reliably ignored by software's rejection criteria.



Figure 9. Optical position measurement with camera and light source.



Figure 10. Applied markers to be detected by the optical system.

Requirements against Wind Tunnel Models

The mass of an unsteady moving model as well as the moments of inertia must be as low as possible to achieve a favorable ratio between the interesting aerodynamic forces and the additional acting forces from mass. On the other hand, the elastic deformation has to be as small as possible. Furthermore, the first Eigenfrequency of the model should be one order of magnitude above the excitation frequency, at least 15 Hz, to avoid excitation of the model by possible higher harmonic rates, see also the comments given below according to Fig. 14c. The best material to meet all these requirements proves suitable CFRP. Using CFRP-Sandwich in that way full-size gliders are built, masses as low as 8 kg for models having wingspans of 2 m can be achieved. Most of the models tested in NWB were manufactured by the plastics workshop of DLR in Braunschweig from carbon fibre composites in moulds. Fig. 11 shows a schematic view of the cross section wing. In order to evaluate the influence of individual components of the tested airplane configuration, such as winglets, vertical or horizontal stabilizer, nacelles, the models are designed in a modular way so that every component of interest can be added to the model, Fig. 12.

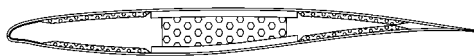


Figure 11. Typical wing cross section.

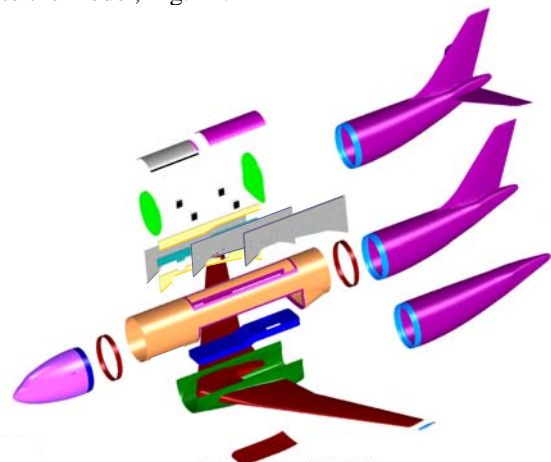


Figure 12. Typical model setup example DLR-F12.

Numerical Approach

The first calculations are based on the panel method VSAERO, a code calculating the nonlinear aerodynamic characteristics of arbitrary configurations in subsonic flow [22], [23]. In an iterative loop with an applied integral boundary layer calculation some viscosity effects can be considered. With this program effects from quasi-steady motions about the body-fixed axis can be calculated.

Recent calculations are based on the solution of the Reynolds-averaged Navier-Stokes solution equations. This is accomplished by adopting a finite volume flow solution method, the DLR TAU code [23], which is characterized by an unstructured mesh concept. The solver is part of the MEGAFLOW project and is presented in detail in [25]. In addition to quasi-steady solutions time-accurate computations are possible. For a brief introduction into the numerical environment please refer to [14].

Generally, there are different approaches to obtain the parts of the dynamic derivatives. Fig. 13 describes as an example the pitching moment due to the pitching motion and the resulting derivative.

The dynamic pitching motion about the mean value α_0 with an amplitude $\Delta\alpha$ generates a hysteresis loop in the aerodynamic response. The bulging out of this hysteresis loop represents the dynamic derivative. In this case the pitching moment is negative (damping) and the direction of the signal is anti-clockwise. The derivative is the sum of two terms:

$$C_{m\dot{\alpha}} = \frac{\partial C_m}{\partial(\partial\alpha/\partial t)} \quad \text{and} \quad C_{mq} = \frac{\partial C_m}{\partial q}.$$

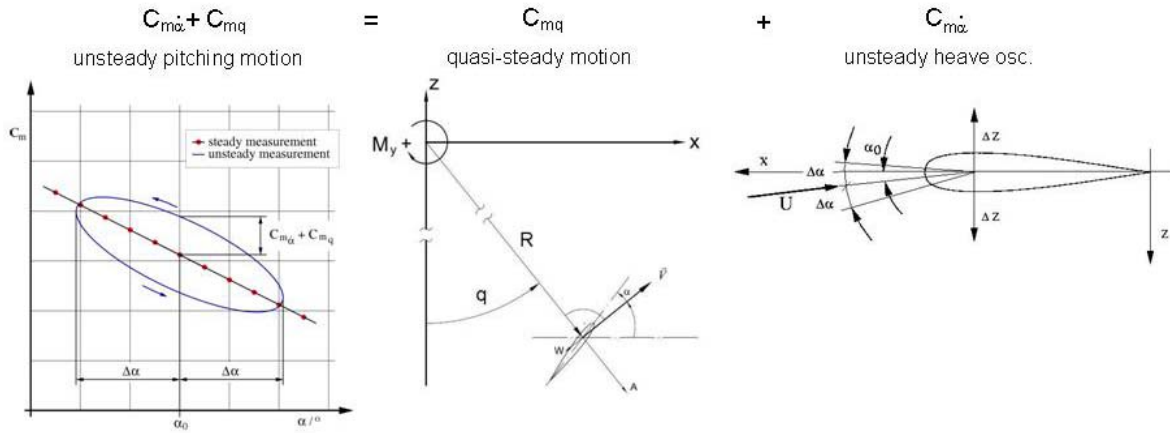


Figure 13. Dynamic derivative of the unsteady pitching motion.

C_{mq} is the quasi-steady term and represents the pitch moment C_m due to constant pitching rates q . After some transient effects at the beginning of the process the resulting forces and moments converge to steady state condition. Calculated motions with different ratios of pitching rate q and lever arm r (see Fig. 13) by constant onflow condition give the $C_{m\dot{\alpha}}$ -term.

$C_{m\dot{\alpha}}$ is an unsteady term. It describes e.g. the influence of a wing tip vortex which reaches the horizontal tailplane after a time delay. The unsteady terms can be obtained by simulating pure heave oscillations.

Results

To illustrate the improvement of the kinematic regarding the quality of motion and its applicability as test rig for dynamic wind tunnel tests Fig. 14a shows for comparison between the OMS and the new MPM in its upper part the measured positions of the wind tunnel model over the time and the corresponding frequency spectrum from a Fourier Analysis during a forced sinusoidal yawing motion. In the right part of Fig. 14a the corresponding measured yawing moment and likewise its derived frequency spectrum are depicted. For an assessment of the fidelity of the motion the forces and moments relevant for the choice of the balance are much more meaningful. As the force and hence the moments involved are straightly proportional to the acceleration the moments curve history can be regarded as the second derivative of the position's curve history.

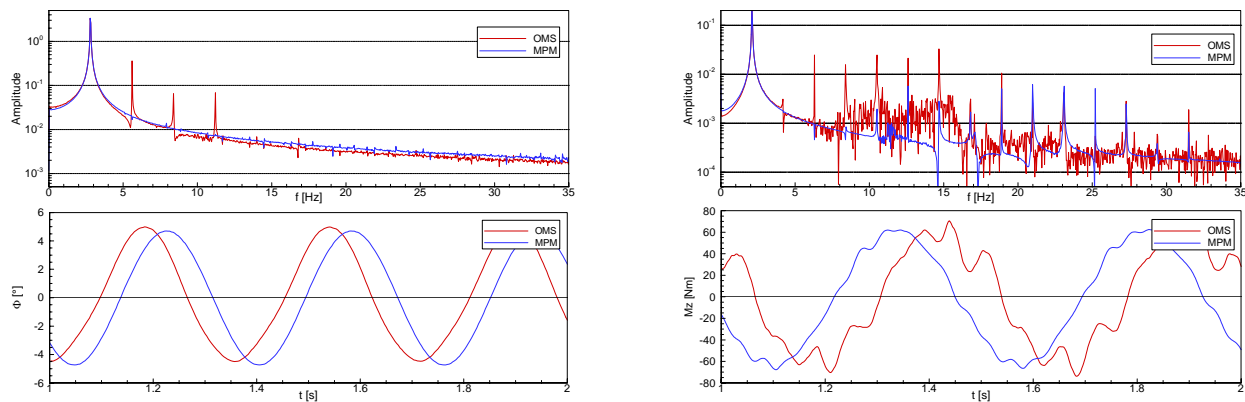


Figure 14a. Yawing motion MPM, $f = 2.1$ Hz.

The position signals of MPM and OMS show a pretty good sinusoidal shape and the frequency spectrum of the position shows only minor differences between the behavior of OMS and MPM. However, the OMS has some higher harmonics of the excited frequency of 2.1 Hz and this is a disadvantage because the acting forces are proportional to the square of the motion's frequency. On the other hand, the comparison of the corresponding measured moments gives distinct differences between the two kinematics. From the frequency spectra the higher harmonics of the MPM are up to one order of magnitude less than that from the OMS, a result of the increased stiffness of the new apparatus.

Since the yawing motion results from the six actuators arranged in parallel manner of the hexapod mechanism the pitching motion is performed by the single seventh axis as a coupled kinematic. Fig. 14b gives an insight into the performance at that pattern of movement and the same good improvement can be recognized. All results shown so far are obtained in wind-off condition.

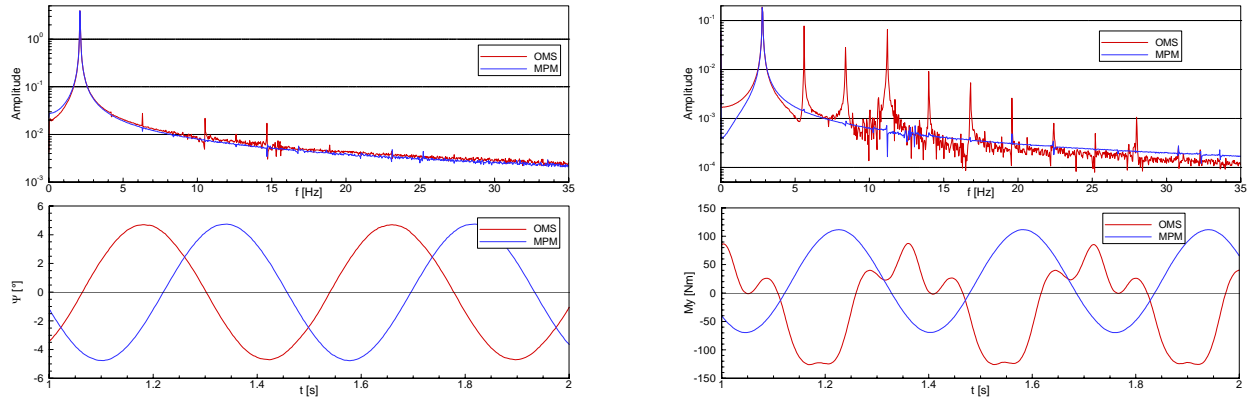


Figure 14b. Pitching motion MPM, $f = 2.8$ Hz.

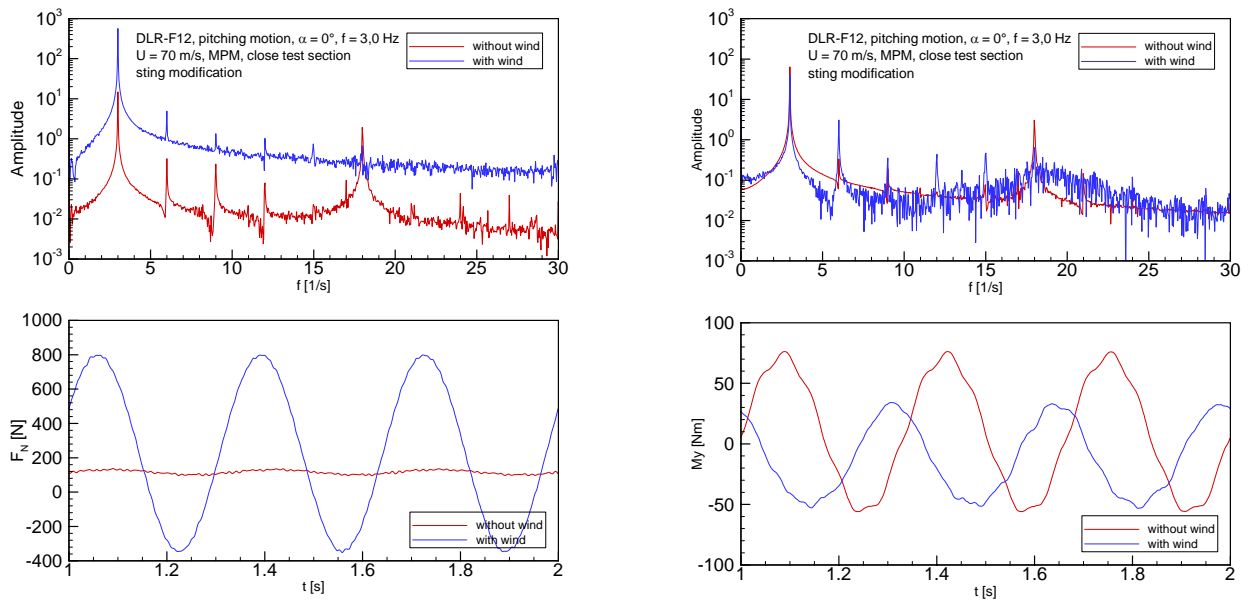


Figure 14c. Pitching motion MPM, $f = 3$ Hz.

To give an impression about the importance of considering the Eigenfrequencies of the complete system a similar test with another model was repeated with 3 Hz forced sinusoidal excitation. The results are shown in Fig. 14c for wind-off and wind-on conditions. The Eigenfrequency of 15 Hz of the DLR-F12 wind tunnel model is considerably visible in the normal force F_N as well as in the pitching moment M_y , admittedly much more in wind-off condition due to favorable damping effects at wind-on condition. Nevertheless, this example makes abundantly clear that the specification of the Eigenfrequency of the model should be carefully reconciled with the requirements of the test program.

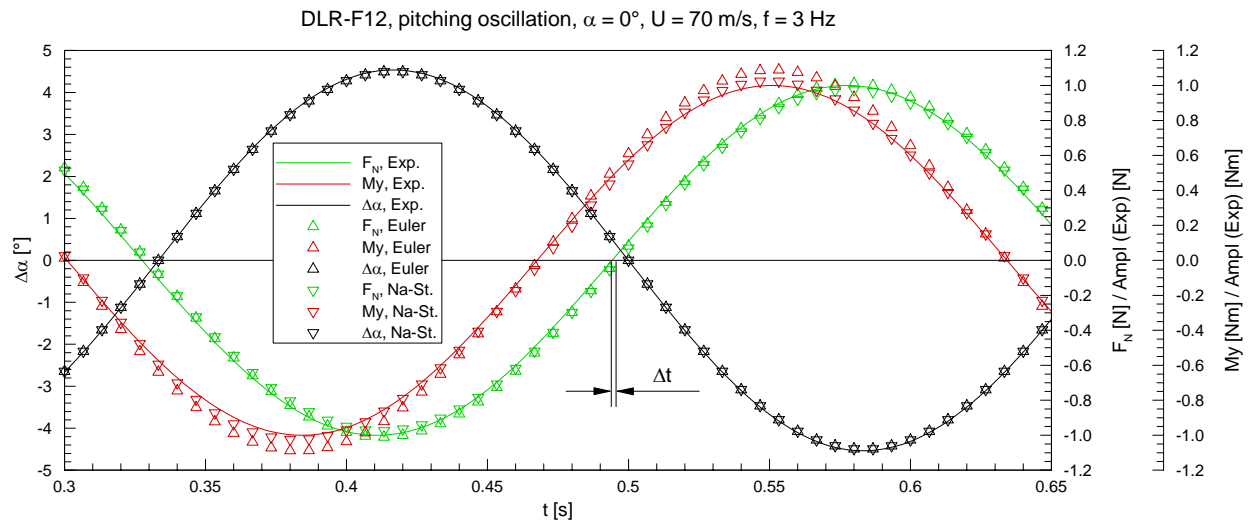


Figure 15. DLR-F12. pitching oscillation, $\alpha = 0^\circ$, $U = 70$ m/s, $f = 3$ Hz.

A comparison between unsteady numerical and experimental results is depicted in Fig. 15. It can be taken from the position curve that at the wind tunnel test the commanded amplitude of $\Delta\alpha = 4.5^\circ$ was only shortly achieved, hence the difference between the amplitude from calculation and experiment. This situation can be seen as an indicative of the importance of a proper position measurement. At first glance the numerical results meet the experimental results of time-dependent lift and pitching moment pretty well, the Navier-Stokes-Solution does it for the pitching moment even slightly better than the Euler-Solution, and the small gap between the input amplitudes might be the reason for the remaining slight differences. But surveying the calculated and the experimental phase between position and force/moment a phase shift of $\Delta t \approx 2$ ms can be recognized and that leads to the question about the sensitivity of the phase and its impact on the quality of the results.

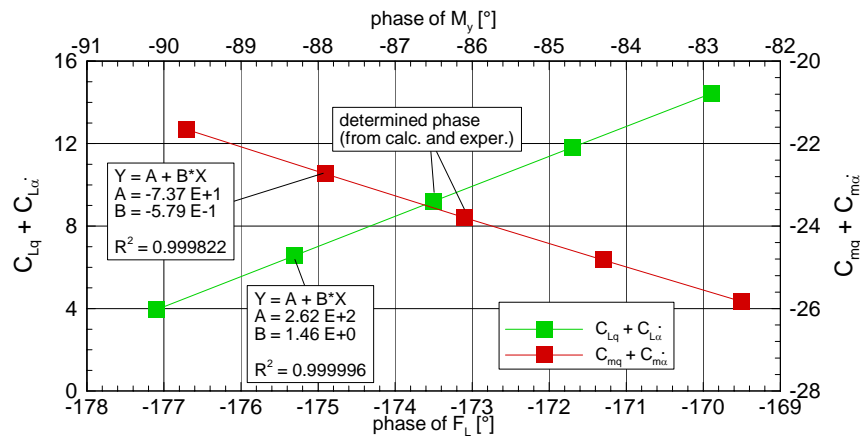


Figure 16. Effect of phase error.

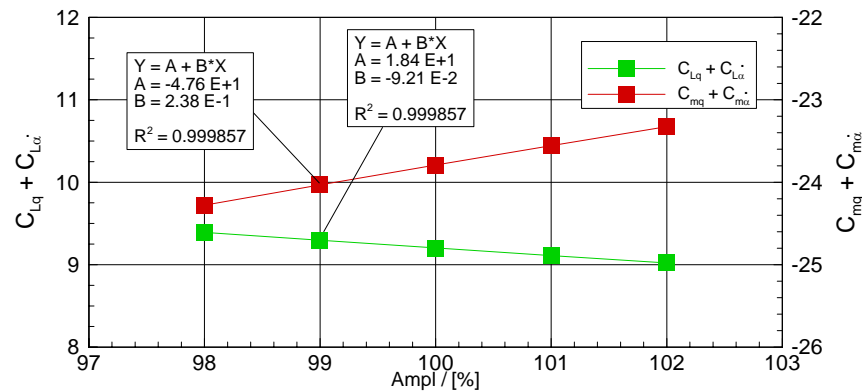


Figure 17. Effect of amplitude error.

Fig. 16 gives the determined phase for the derivatives for lift and moment coefficients due to a pitching motion. It is easy to shift the phase in the result records to get some insight regarding the sensitivity. It comes out that already minor changes in the phase lead to considerable changes in the coefficients. For example 1° phase shift leads to a change in the lift coefficient of about 1.5 or about 15% respectively. It can also be derived that the sensitivity to the pitch damping coefficient is by three times smaller. This interrelation holds true for numerical as well as for experimental results and makes clear that great care has to be taken with regard to the estimation of the phase relationships. Corresponding to the previous procedure the influence of the amplitude can also be evaluated. However it can be taken from the example in Fig. 17 that a false determination of the amplitude leads to only minor effects in the evaluation of the derivatives.

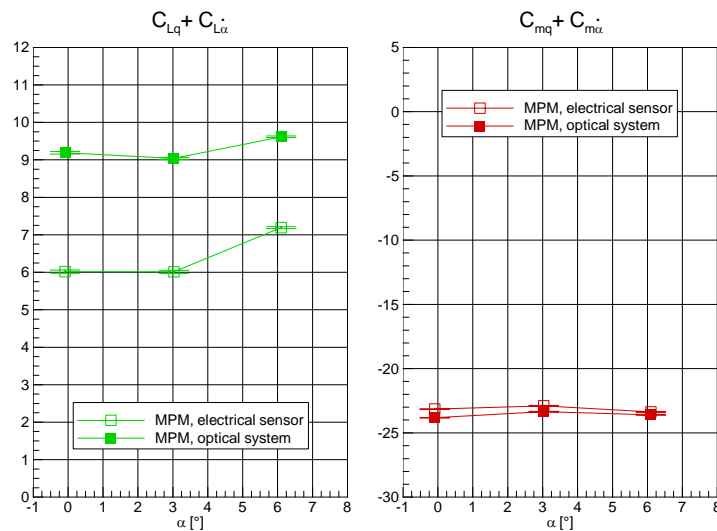


Figure 18. Impact of different pos. measurement techniques on the evaluated derivatives, pitching motion.

Fig. 18 gives for comparison the impact of two different position measurement techniques on the evaluated derivatives again for the pitching motion showcase. One technique is the aforementioned video system that detects the attitude of the model directly and the other is the described electrical sensor that determines the position of the model, as described in Fig. 8, in direct manner. Both techniques were applied simultaneously during one and the same test run. In the results a clear difference of 30% is visible in the lift coefficient and here the influence of the

detected phase and amplitude respectively is visible. The arguments for the optical system are the more reliable prediction of the amplitude as all deformation effects from the testrig can be neglected. That is not the case for the electric sensor as here all deformations between the sensor and the model have to be known. Concerning the phase relationships laboratory tests showed an uncertainty of less than one ms for both techniques, nevertheless with slight advantages for the electrical sensor as this device can be measured with the identical amplifiers than in usage for the balance signals while the video camera can be regarded as a complete separate system. At 3 Hz one ms is equivalent of an error of one degree. Again the difference between the results for the lift due to the pitch oscillation and for the pitch damping is about three times higher.

In Fig. 19a the comparison of various Euler results for the DLR-F12 configuration are shown and the influence of the quasi-steady shares C_{Lq} and C_{mq} as well as of the unsteady shares from heave oscillation $C_{L\dot{\alpha}}$ and $C_{m\dot{\alpha}}$ can be taken. The effects from the unsteady heave oscillation show only minor influence upon the lift due to pitch oscillation while the quasi-steady part is the dominant one. This is typical for the DLR-F12 configuration and is not always the case, as shown in [14], with calculations on a generic wing/tail combination.

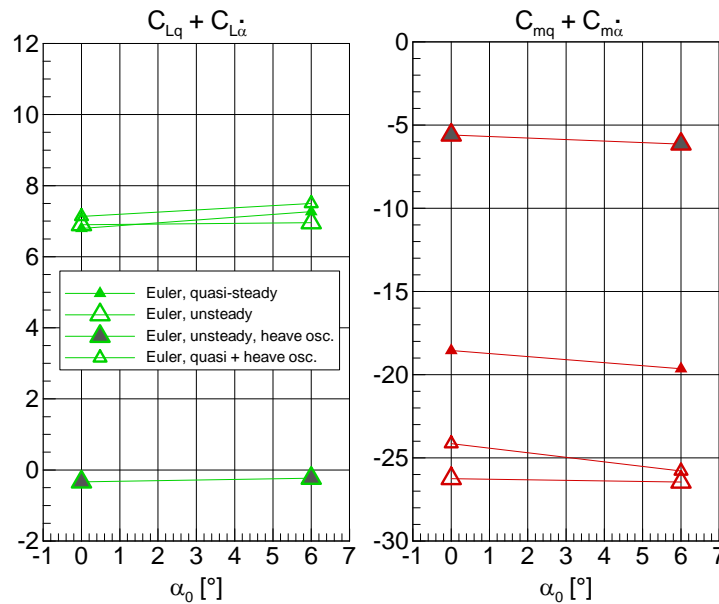


Figure 19a. Different shares of derivatives for Euler results, DLR-F12.

The pitch damping behavior however on the right hand side of Fig. 19a shows an evident influence of the unsteady (heave) $C_{m\dot{\alpha}}$ -term of about 20% and is not negligible. Adding the quasi-steady solutions and the coefficients due to the heave oscillation results gives a sum that is in very good agreement with the full unsteady pitching motion simulation results.

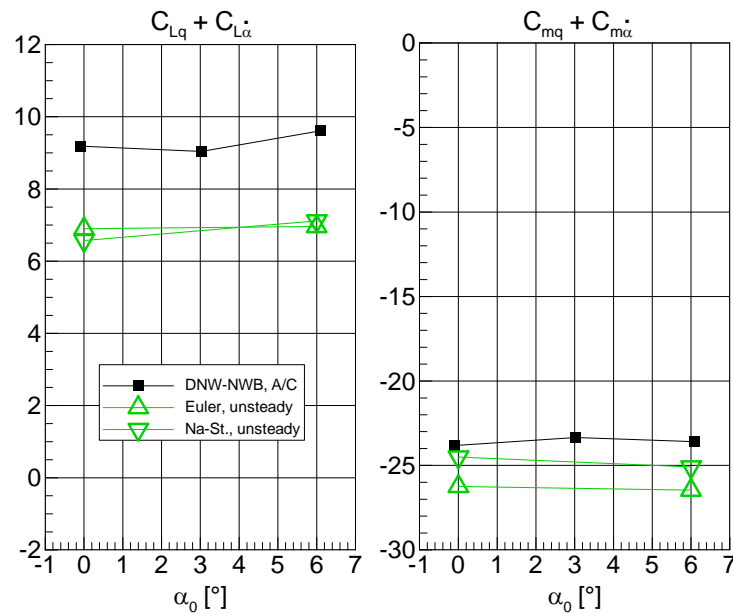


Figure 19b. Comparison of numerical and experimental results at the DLR-F12.

Fig. 19b shows unsteady Euler and Navier-Stokes solutions to get information about the viscous effects. The plot turns out some minor effects and a comparison with experimental data gives still deviations of about 20% in lift coefficient while the results for the pitch damping correlates pretty well. Here again the deviation is about three times smaller than for the lift coefficient and the reason for the remaining discrepancies might be again uncertainties in the prediction of the phase in the magnitude of 1 – 2ms.

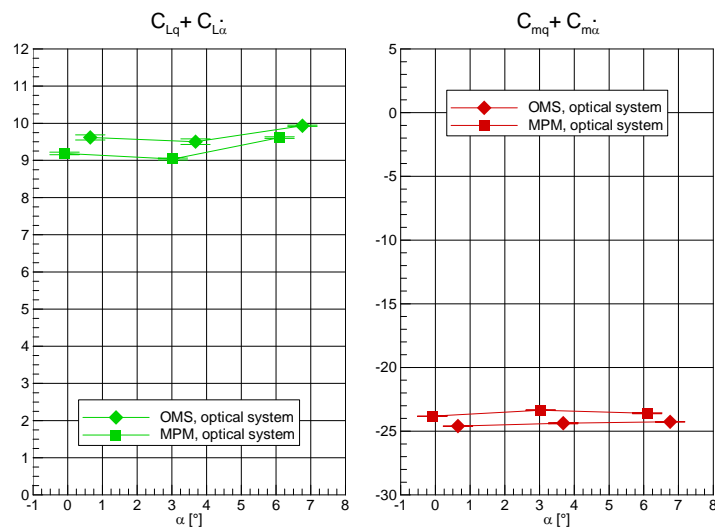


Figure 20. Experimental results from OMS and MPM on the DLR-F12.

Fig. 20 gives a comparison of results with the very same model from the positioning mechanism MPM and its predecessor OMS, again exemplarily for the pitching motion. Due to the improvements regarding stiffness and

precision of the apparatus the experimental data are shifted slightly closer to the calculated predictions, nevertheless still with a small gap.

Outlook

At all numerical investigations and the data evaluations so far it was acted on the assumption of an ideal rigid model without deformation. First work was conducted to evaluate the error due to effects caused by twist and bending of the model's wing. For this purpose a 3D video system with two Mikrotron CMOS video cameras was used for stereo pattern recognition of distinct applied markers on the wing, see Fig. 21.

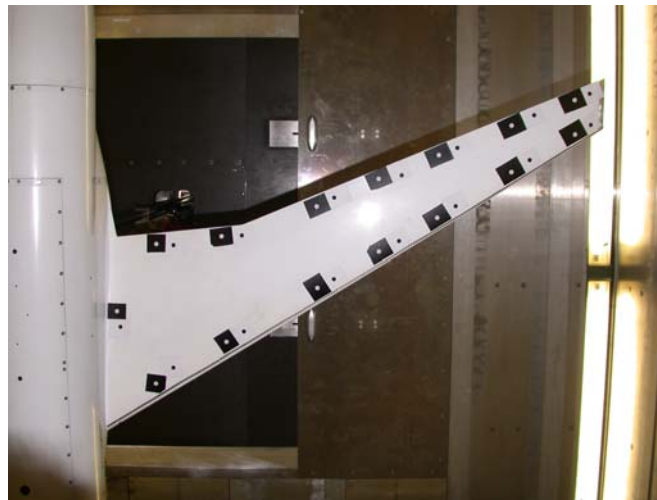


Figure 21. Applied markers for stereo pattern recognition.

The accuracy obtained at that test is about 0.1 mm in lateral direction. The system is described in [26] in more detail. The result is illustrated in Fig. 22. The maximum deflection is 7mm and twist is 0.4° at the wing tip. These experimental results meet the predicted design points pretty well. Very first numerical results from quasi-steady VSAERO calculations with a generic rigid 'flight' shape with a bended wing without twist are depicted in Fig. 23 for the pitch again. The outcome is a considerable shift of the results into the expected direction. From the previous experiences it can be assumed that with more complex and accurate calculations the predicted results will fit again closer to the experimental results.

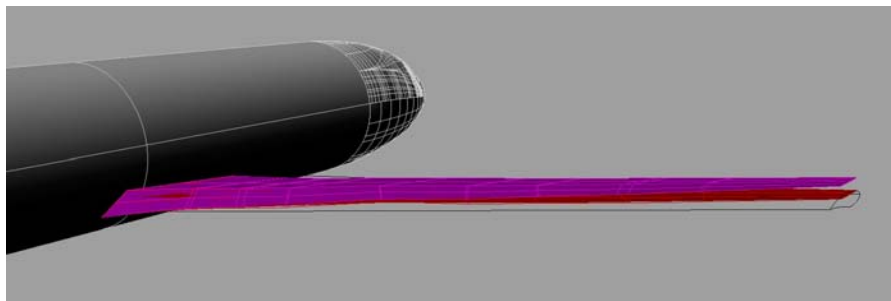


Figure 22. Measured wing deformation of DLR-F12 at constant $\alpha = 10^\circ$, $U_\infty = 56$ m/s.

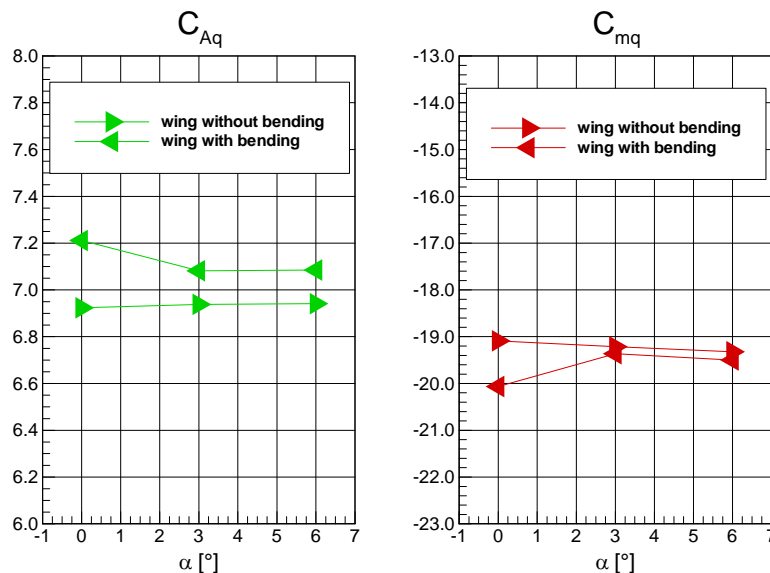


Figure 23. DLR-F12 geometry, VSAERO, inviscid solutions.

The further step will be an investigation of a new elastic wind tunnel model and the determination of the unsteady wing shape during the motion. On the other hand the numerical investigations have to proceed with multidisciplinary codes with coupled aerodynamic-structural solvers to address all parameters necessary for a proper prediction of the unsteady aerodynamics of maneuvering aircraft.

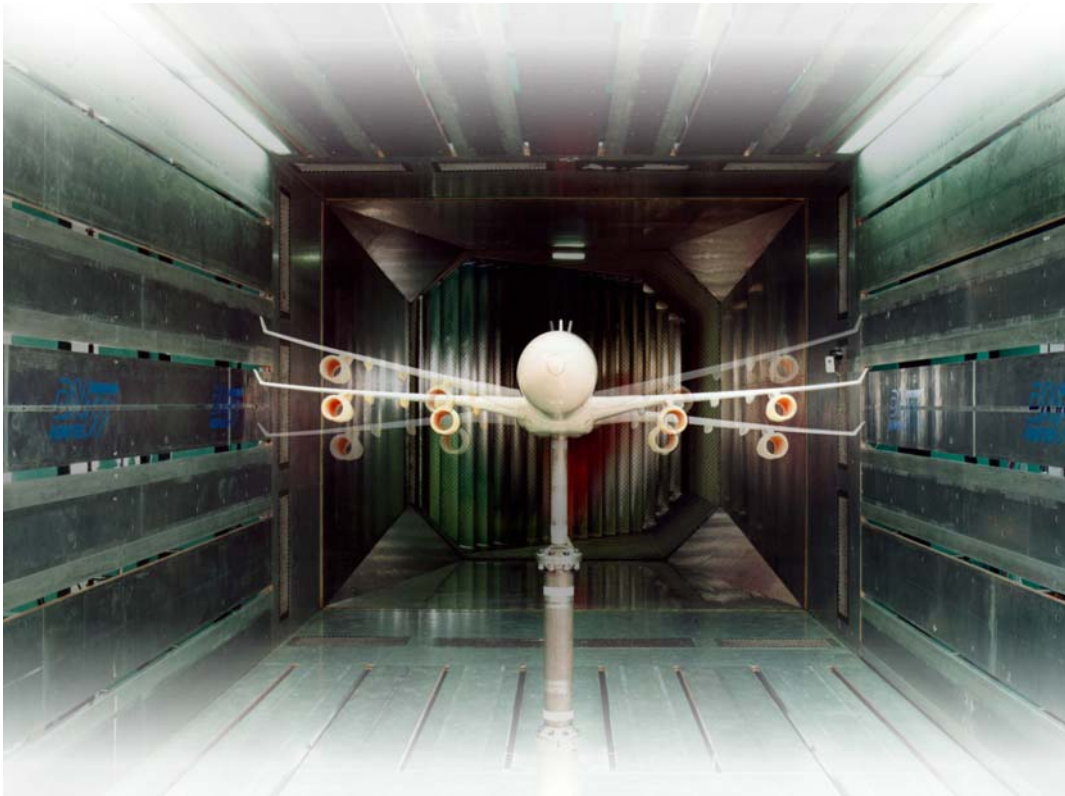
In addition, measurements of the steady and unsteady pressure distributions using the pressure taps of the DLR-F12 full configuration are necessary for the validation process.

References

- [1] Dynamic Stability Parameters, *AGARD-CP-235*, Athens, May 1978 (November 1978).
- [2] Review of Techniques for Determination of Dynamic Stability Parameters in Wind Tunnels, pp. 3-1 to 3-28, 1981.
- [3] K.J. Orlik-Rückemann: Dynamic Stability Testing of Aircraft – Needs versus Capabilities, *Prog. Aerospace Sci.*, Vol. 16, No. 4, pp. 431 to 447, 1975.
- [4] Unsteady Aerodynamics – Fundamentals and Applications to Aircraft Dynamics, *AGARD-CP-386*, Göttingen, May 1985 (November 1985).
- [5] Manoeuvring Aerodynamics, *AGARD-CP-497*, Toulouse, May 1991 (November 1991).
- [6] Rotary-Balance Testing for Aircraft Dynamic, *AGARD-AR-265*, Report of WG 11, 1990.
- [7] Cooperative Programme on Dynamic Wind Tunnel Experiments for Manoeuvring Aircraft, *AGARD-AR-305*, Report of WG 11, October 1996.
- [8] Verification and Validation Data for Computational Unsteady Aerodynamics, *RTO TR-26*, Report of RTO-WG-003 (AGARD WG-22), October 2000.

- [9] T. Loeser: Dynamic Force and Pressure Measurements on an Oscillating Delta Wing at Low Speeds, *IB 129-96/7*, Deutsche Forschungsanstalt für Luft- und Raumfahrt (DLR), includes Addendum.
- [10] J. von der Decken, E. Schmidt, B. Schulze: On the Test Procedures of the Derivative Balances used in West Germany, *AGARD-CP-835*, pp. 6-1 to 6-17, 1978.
- [11] X. Hafer: Wind Tunnel Testing of Dynamic Derivatives in W-Germany, *AGARD-CP-235*, pp. 5-1 to 5-22, 1978.
- [12] T. Loeser, A. Bergmann: Development of the Dynamic Wind Tunnel Testing Capabilities at DNW-NWB, *AIAA-2003-0453*, 41th AIAA Meeting, Reno, 2003.
- [13] A.-R. Huebner, T. Loeser: Methods for Determination of the Unsteady Aerodynamic Derivatives for Transport Aircraft Configurations, *RTO-AVT-123*, Budapest, 2005.
- [14] A.-R. Huebner: Experimental and Numerical Investigations of Unsteady Aerodynamic Derivatives for Transport Aircraft Configurations, *AIAA-2007-1076*, 45th AIAA Meeting, Reno, 2007.
- [15] M. Rein, G. Hoehler, A. Schuette, A. Bergmann, T. Loeser: Ground-based Simulation of Complex Maneuvers of Delta-wing Aircraft, 25th AIAA Aerodynamic Measurement Technology and Ground Testing Conference, San Francisco, 2006.
- [16] A.-R. Huebner, T. Loeser: Recent Improvements in the Measurement of Aerodynamic Damping Derivatives, in: Wagner et al. (Eds): *New Results in Numerical and Experimental Fluid Mechanics III*, Springer, Berlin, 2002.
- [17] D.I. Greenwell: Analysis of a Six Degree-of-Freedom Dynamic Wind Tunnel Test Rig Mechanism Based on the Stewart Platform, *AS/HWA/TR96102/1*, DERA, Farnborough, December 1996.
- [18] A. Wiegand, S. Weikert: Vorrichtung zur räumlichen gesteuerten Bewegung eines Körpers in drei bis sechs Freiheitsgraden, Internationale Patentanmeldung WO 97/22436, 19.12, 1996.
- [19] M. Honegger: Adaptive Control of the Hexaglide, a 6 DOF parallel manipulator, Robotics and Automation, Proceedings, IEEE International Conference, pp. 543-548, Vol. 1, 1997.
- [20] A. Bergmann et al.: MPM, *USA Patent Application Pub.No. US 2006/0254380 A1*, November 2006.
- [21] R.H.G. Mueller, K. Pengel: Blade Deflection Measurement at Low Noise ERATO Rotor, 26th Europ. Rotorcraft Forum, The Hague, Netherlands, paper 104, 2000.
- [22] J.K. Nathmann: VSAERO a Computer Program Characteristics of Arbitrary Configurations, Analytical Methods Inc. Redmond, Washington, November 1997.
- [23] B. Maskew: Predicting Aerodynamic Characteristics of Vortical Flows on Three-Dimensional Configurations Using a Surface-Singularity Panel Method. Analytical Methods Inc. Redmond, Washington, July 1983.
- [24] N. Kroll, C.-C. Rossow, K. Becker, F. Thiele: MEGAFLOW – A Numerical Flow Simulation System, 21st ICAS, Melbourne, *ICAS-98-2.7.4*, 1998.
- [25] M. Galle, T. Gerhold, J. Evans: Technical Documentation of the DLR TAU-Code, *DLR-IB 233-97/A43*, 1997.
- [26] T. Loeser, A. Bergmann: Capabilities of Deployment Tests at DNW-NWB, *RTO-AVT-133*, pp. 13-1 to 13-11, Lituania, 2006.

Integrated Experimental and Numerical Research on the Aerodynamics of Unsteady Moving Aircraft



A. Bergmann



A. Hübner



- Motivation
- Test Setup
- Numerical Approach
- Typical Results
- Outlook

Evaluation of flight characteristics is still an issue!

→ Evaluate and describe the aerodynamics in the manoeuvring flight regime

Dynamic Derivatives are required for

- Prediction of flight dynamics (candidate conf., design FCS, knowledge S&C)
- Loads prediction for structural design of aircraft components
- Data-Set for CFD validation process

Common method (for transport aircraft)

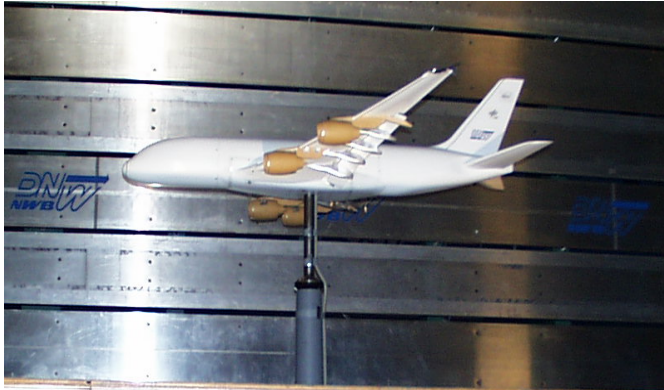
- Assessment from simple handbook methods
- Application of corrections (from flight tests)

Dynamic Stability Testing of A/C NEEDS vs. CAPABILITIES	Low α (Transport aircraft)	High α (Space Shuttle, Concorde, Fighter aircraft)
Flow	mainly linear, often well known	strong non-linear effects (separation, transition, vortex shedding, etc.)
Analytical prediction of dynamic derivatives	easy (linear potential methods and various approximations often acceptable)	very difficult (highly non-linear, often speculative, approximations risky)
Magnitude of dynamic derivatives	small	sometimes very large, varying sign
Variation of dynamic derivatives with α	small	sometimes very rapid
Effect of dynamic derivatives on flight trajectory and on stability and control	insignificant or at least constant and well-known	sometimes very large, may often be significant.



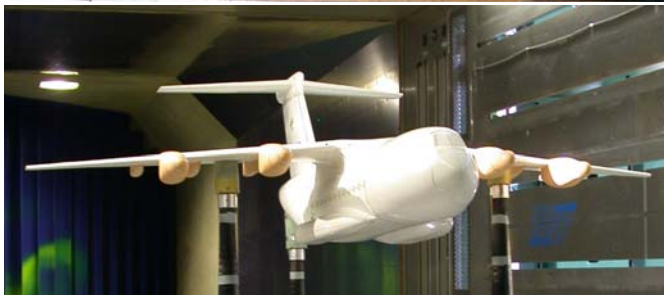
Changing interest in dynamic derivatives – high α vs. low α

Today's Situation



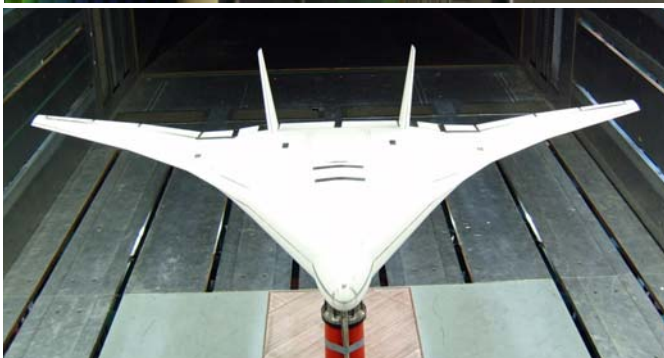
A380

- relative short lever arm of tail unit
- larger taper ratio
- non-circular cross section



A400M

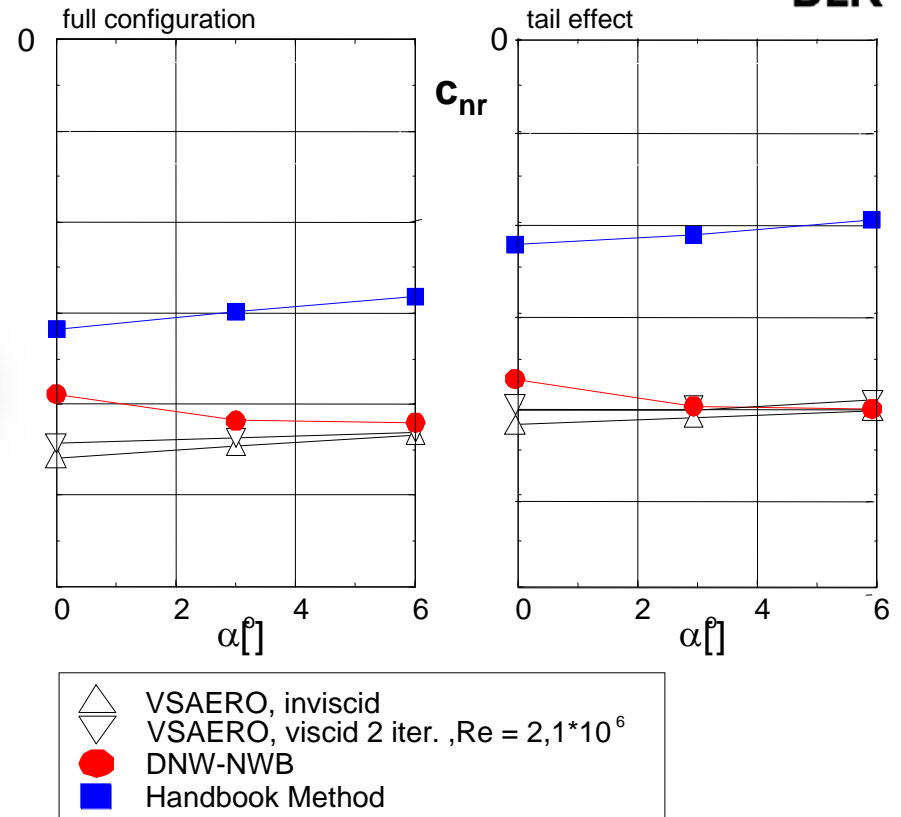
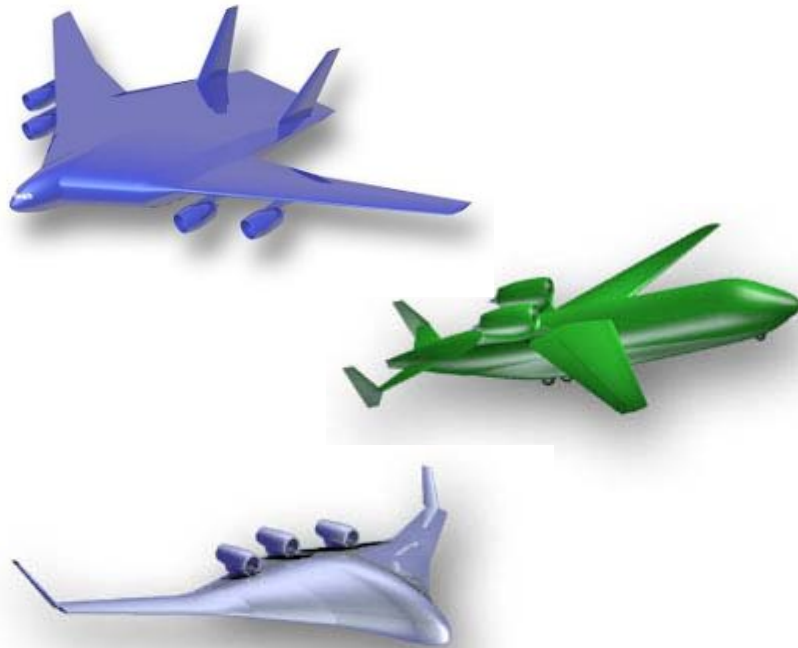
- tail ramp
- sponsons
- T-tail



BWB

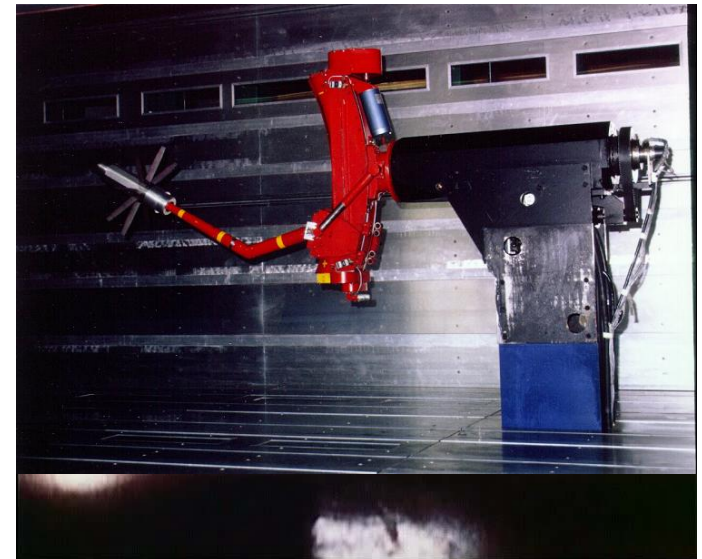
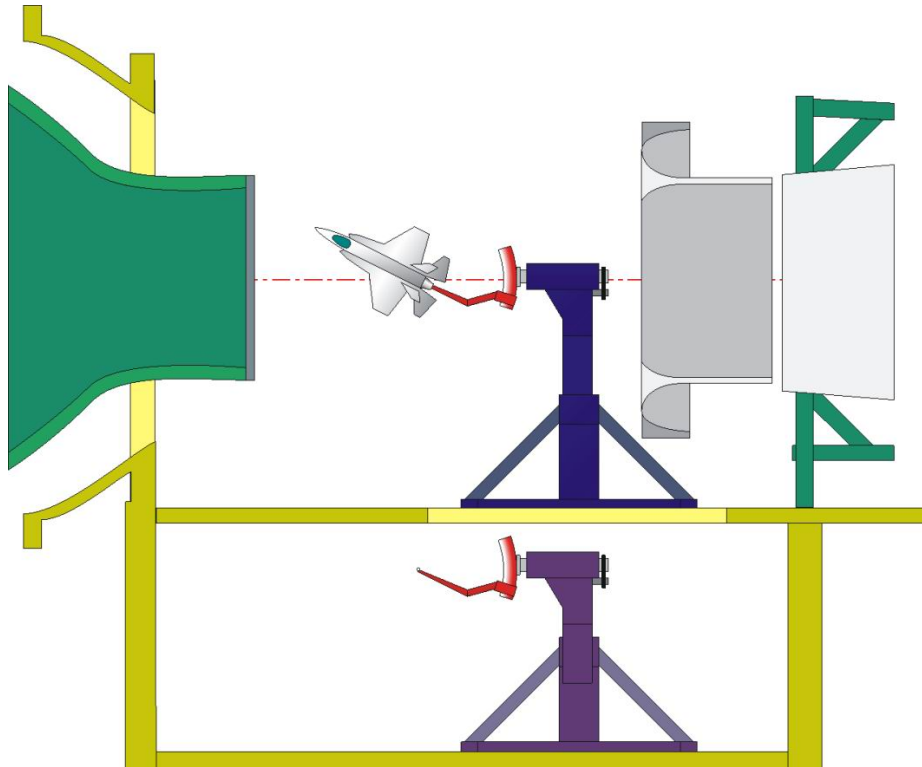
- hybrid shape
- short lever arms, small damping

Possible Future Situation



For new configurations semi empirical methods are not accurate as required
 → High fidelity tools
 → Improved data accuracy

Rotary-Balance of DNW-NWB



Mobile Oscillatory Derivative Balance (MOD) since 1970

Serial kinematic structure:

Number of DoF is achieved by serial arrangement of the corresponding number of linear and rotative axes

The bottom-most axis of movement has to carry the weight of all those lying above it.

→ NOT well suited for the requirements

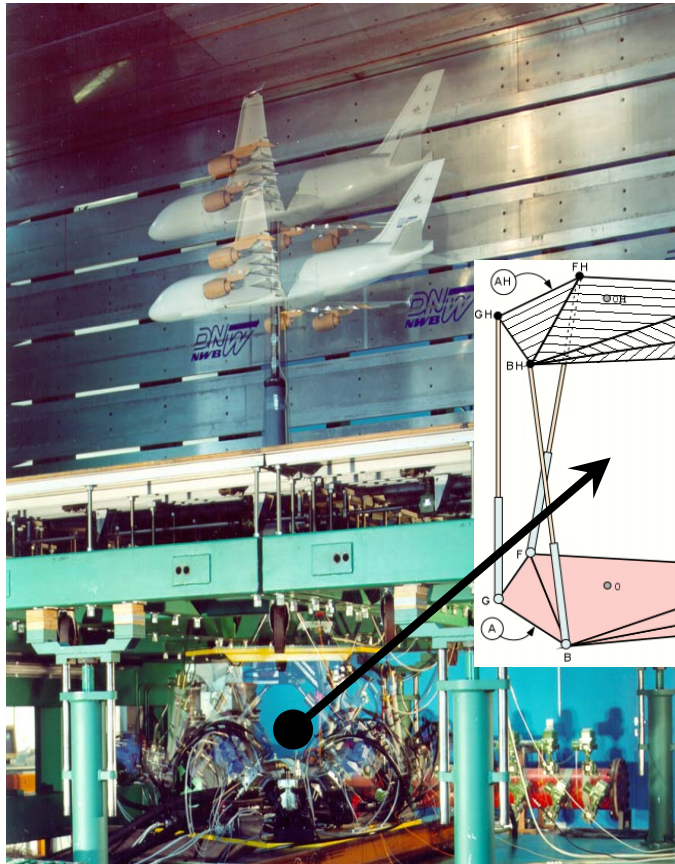
- > high stiffness

- > low mass

The errors (thermal, geometric, caused by loads) of movement of all axes are added



Oscillatory Motion System (OMS) since 2000



Parallel kinematic structure
based on Stewart Platform

6 telescope like, driven legs \rightarrow 6DoF

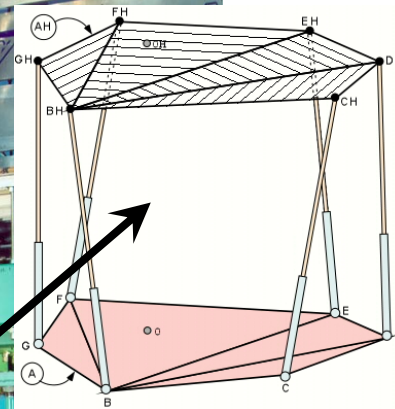
Masses to be moved are smaller

Errors not added

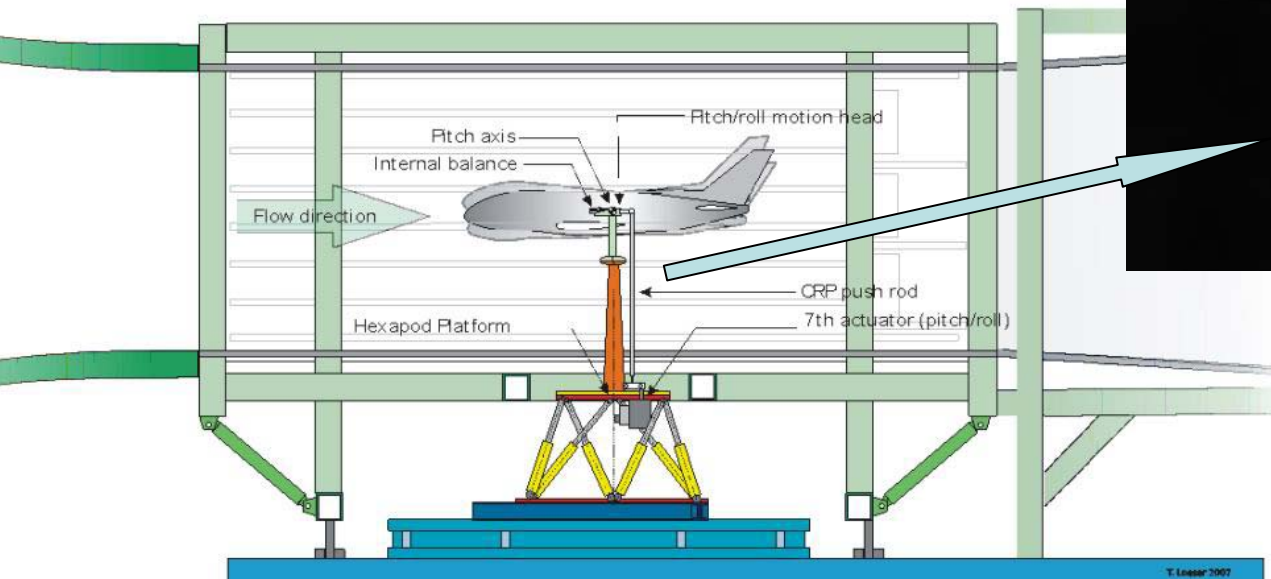
Only forces in axial direction
of the legs (largest stiffness)

Available working space smaller
compared to machine - size

Hydraulically driven



Use of the Hexapod System OMS...



...in combination with a gear box in the fuselage as coupled kinematics

Approach since 2003:

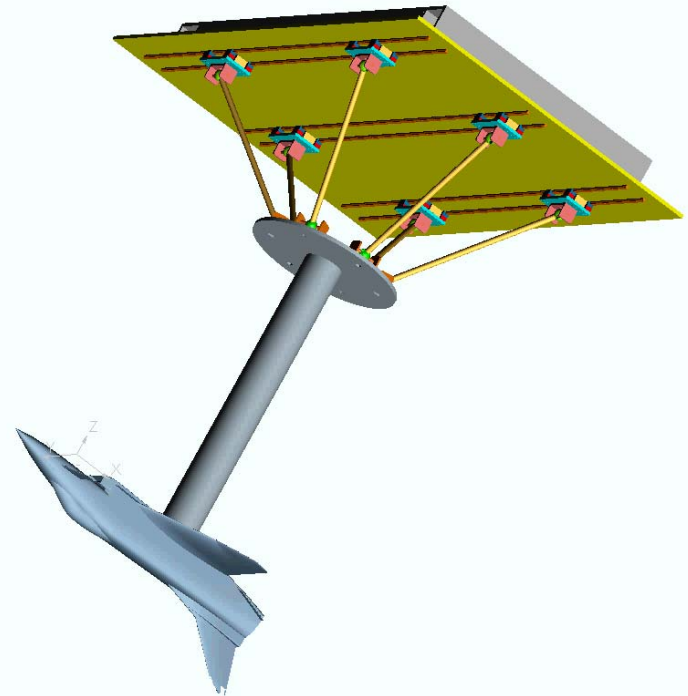
Investigation of an existing prototype of milling machine based on parallel kinematics

goal: develop an optimized system to meet the requirements of W/T model support

Design and build a W/T dynamic test rig to investigate manoeuvring characteristics of future aircraft

→ 6DOF

→ representative rates / ampl.



Principle of Rod kinematic
6 rods with constant length
rail guides, electrically driven

6 DoF

Workspace (long., lateral, heave): 1100mm, 300mm, 500mm

Pivoting angles of	- 5° to + 5° for rolling, accuracy	< 0.005°
	-15° to + 7° for pitching	< 0.01°
	-10° to +10° for yawing	< 0.005°

Near constant and high stiffness all over the workspace

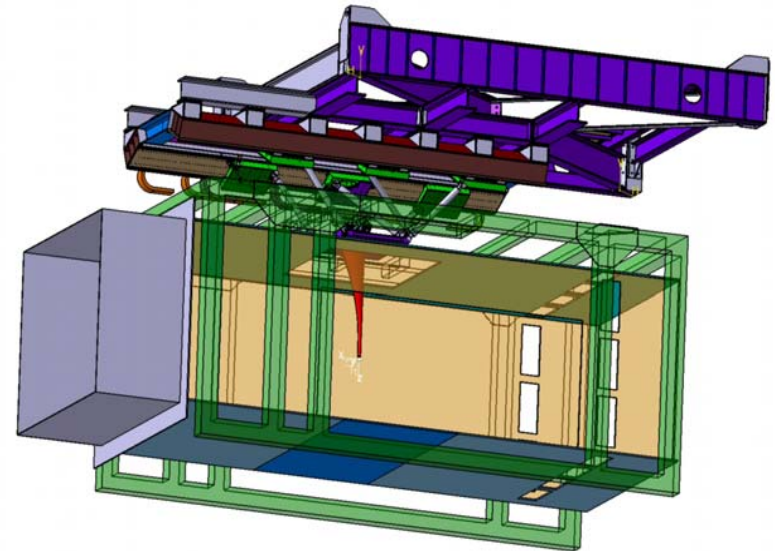
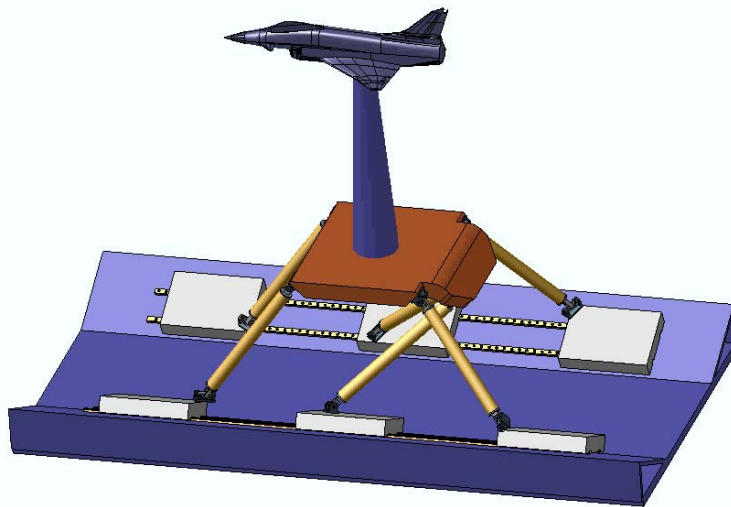
First eigenfrequency > 20 Hz

Max acceleration 2.5 g

Oscillatory Motion of the model in the modes

Yawing, Pitching, Rolling, (Heave) up to 3 Hz with 5°(60mm) Amplitude

Max payloads	Fx / Fy / Fz	1500 / 1000 / 5000 N
	Mx / My / Mz	500 / 1000 / 600 Nm

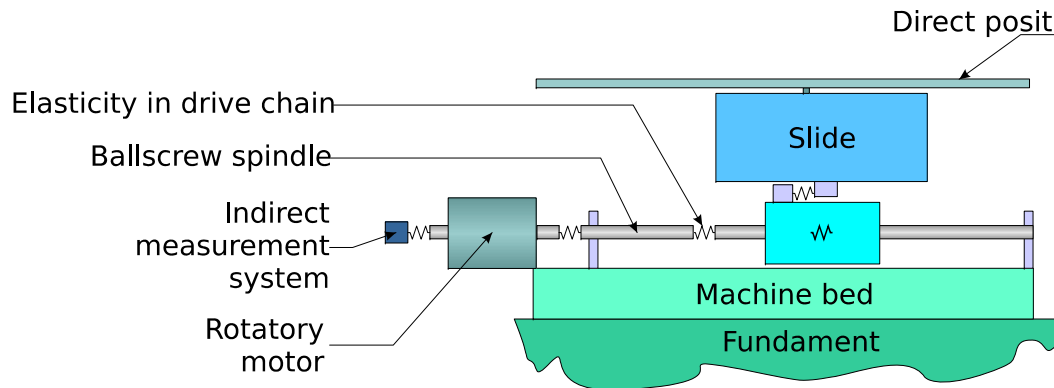


- Use of conventional standard components → cheaper
- Use of six constant length rods made from CRP → small masses, high stiffness ($1400\text{N}/\mu\text{m}$)
- Reduction to two parallel tracks → unique design of a parallel kinematic, cheaper, simpler
- Use of linear electromagnetic motors → highest accuracy and highest dynamic

Comparison:

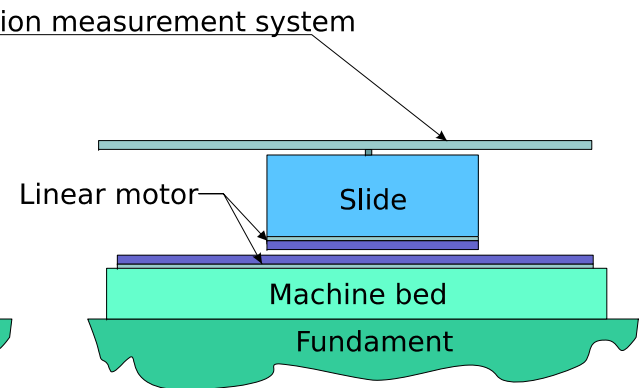
Conventional ballscrew drive

Indirect force build-up
⇒ reduced dynamics



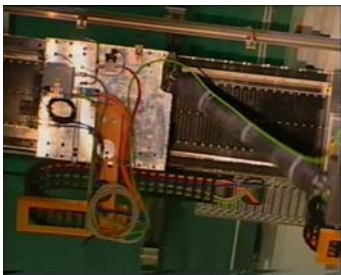
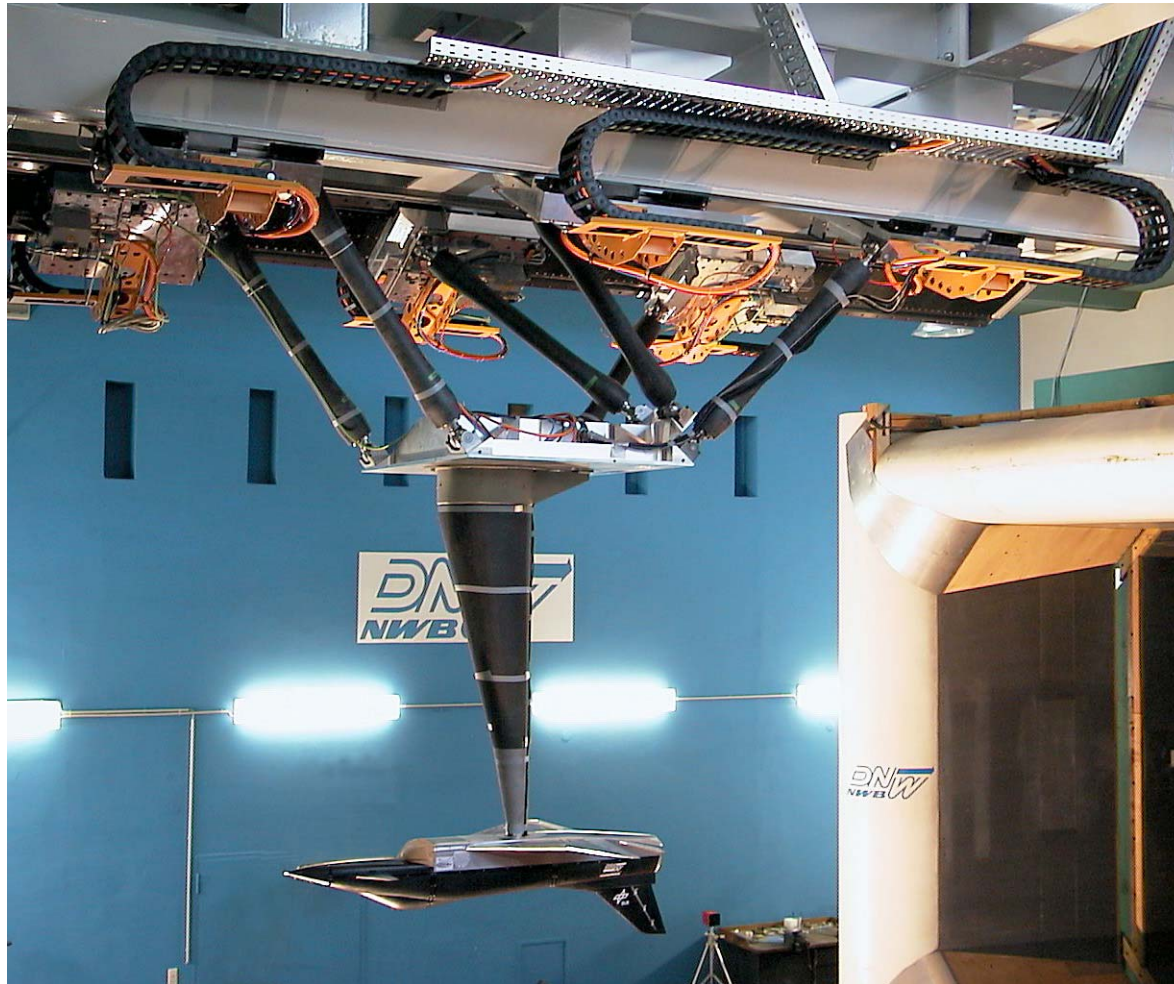
Linear direct drive

Force build-up directly at the slide
⇒ **highest dynamics**



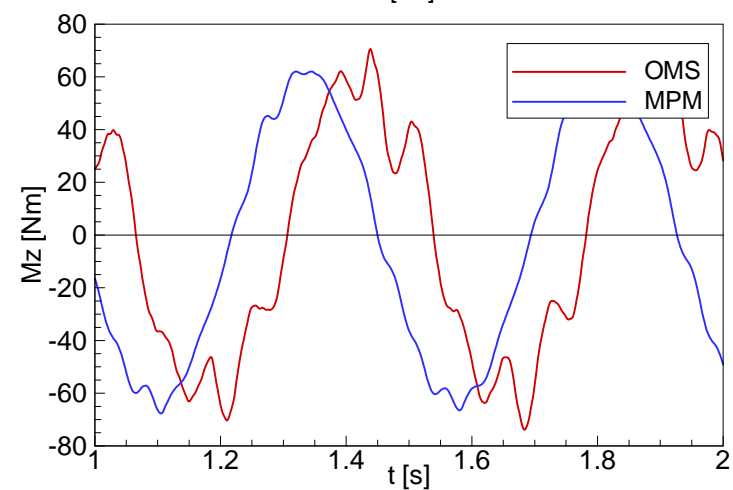
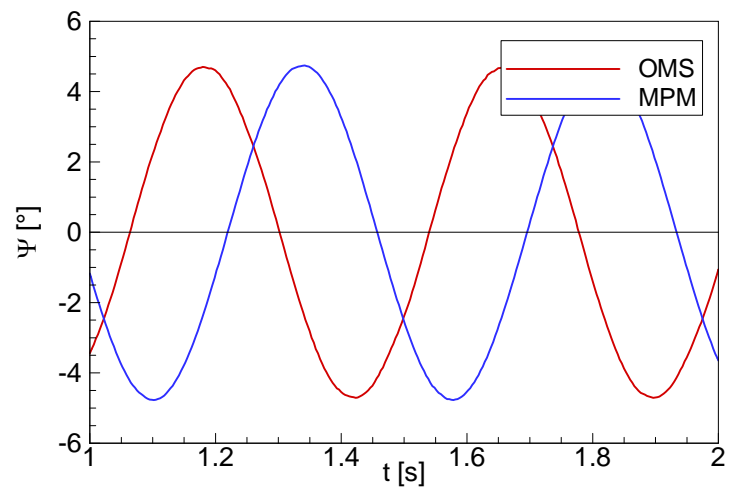
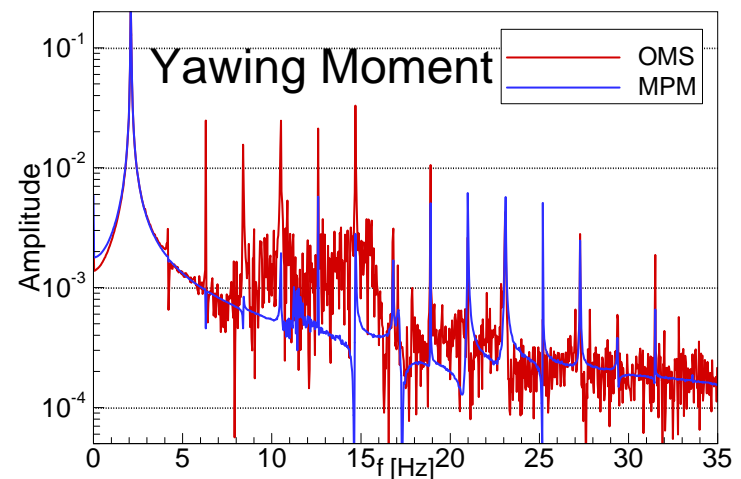
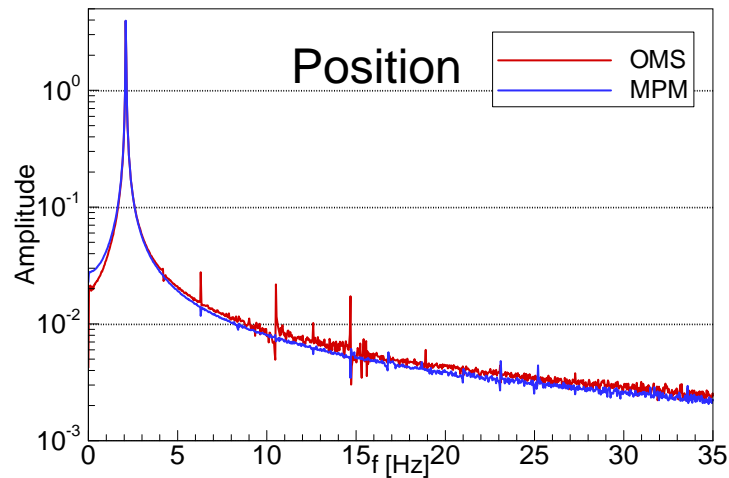
Max Force: 20,700 N
Velocity at F_{\max} up to 6 m/sec

The unique MPM for dynamic testing in the open testsection of NWB



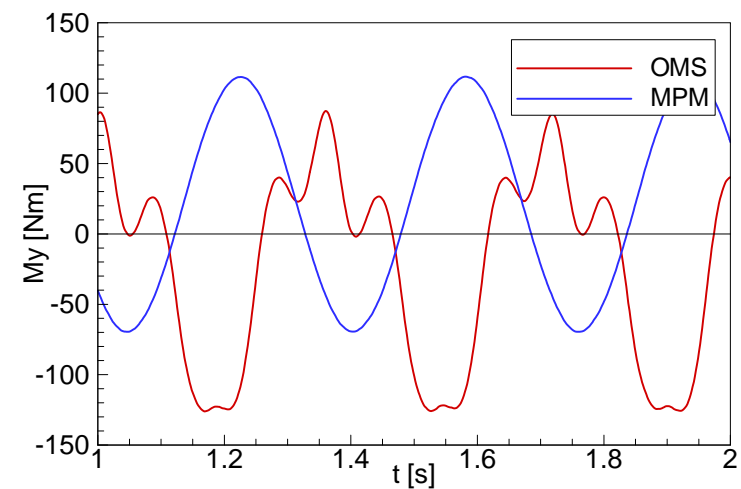
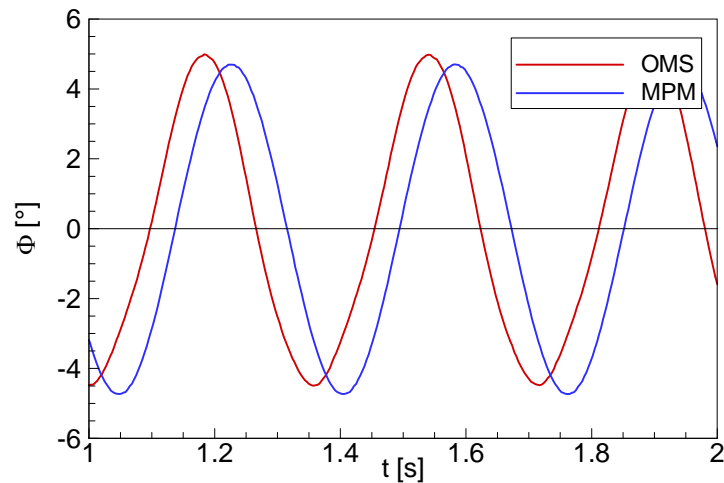
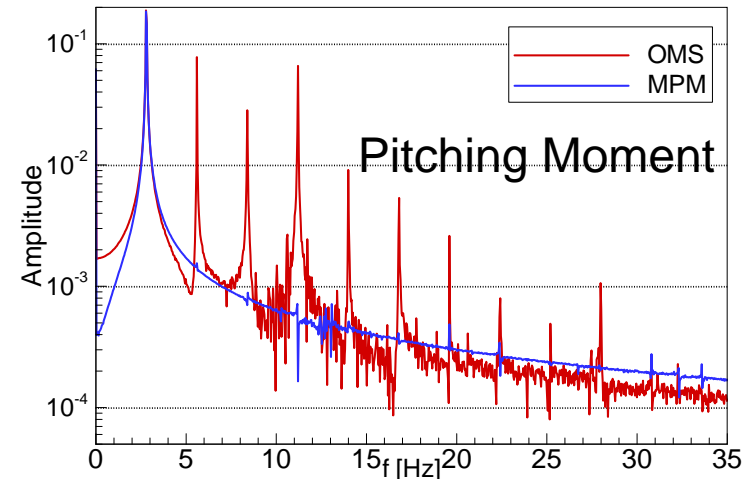
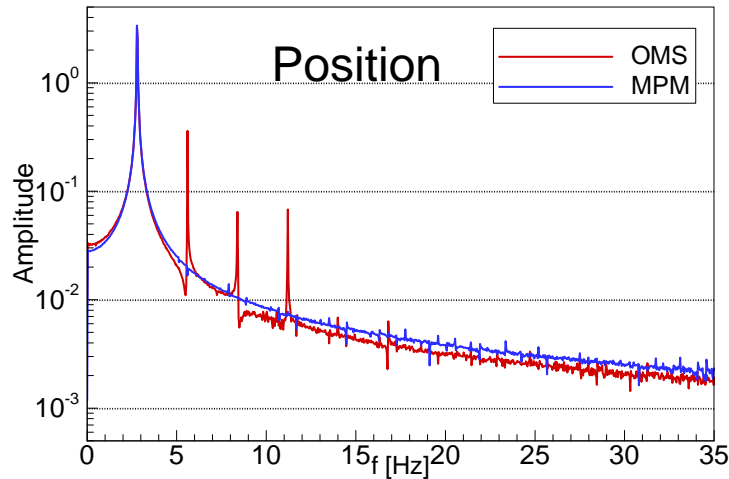
Comparison OMS vs. MPM

Yawing Motion, $f=2.1\text{Hz}$



Comparison OMS vs. MPM

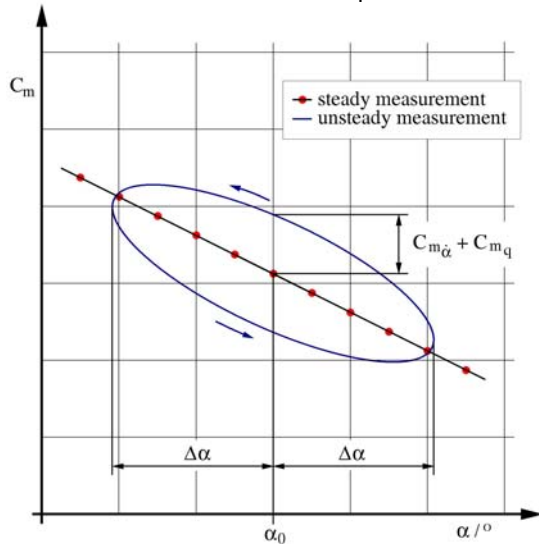
Pitching Motion, $f=2.8\text{Hz}$



Dynamic Derivatives

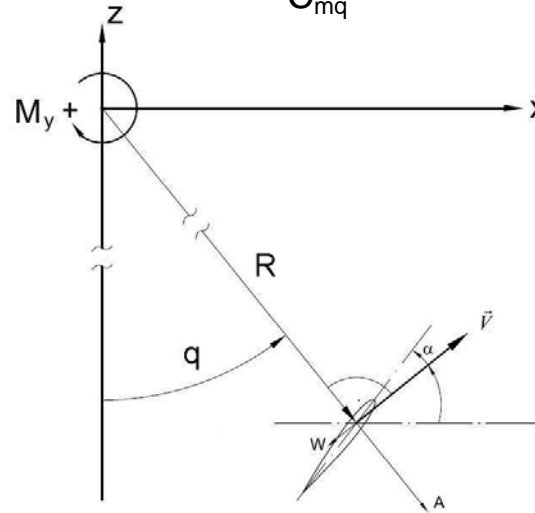
unsteady pitching motion

$$C_{m\dot{\alpha}} + C_{mq}$$



= quasi-steady motion

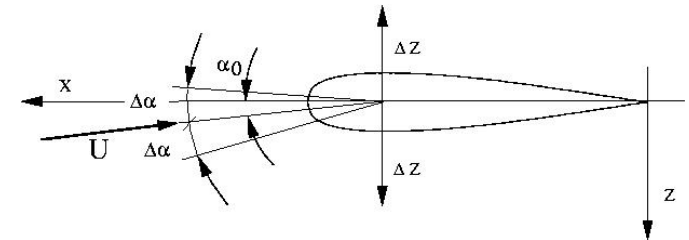
$$C_{mq}$$



+

unsteady heave osc.

$$C_{m\dot{\alpha}}$$



Roll

$$C_{lp}$$

$$C_{np}$$

$$C_{Yp}$$

$$= f(p)$$

Pitch

$$(C_{D\dot{\alpha}} + C_{Dq})$$

$$C_{L\dot{\alpha}} + C_{Lq}$$

$$C_{m\dot{\alpha}} + C_{mq}$$

$$= f(\dot{\alpha}, q)$$

Yaw

$$C_{lr} - C_{l\dot{\beta}}$$

$$C_{nr} - C_{n\dot{\beta}}$$

$$C_{Yr} - C_{Y\dot{\beta}}$$

$$= f(\dot{\beta}, r)$$

Heave osc.

$$C_{W\dot{\alpha}}$$

$$C_{A\dot{\alpha}}$$

$$C_{m\dot{\alpha}}$$

$$= f(\dot{\alpha})$$

Lateral osc.

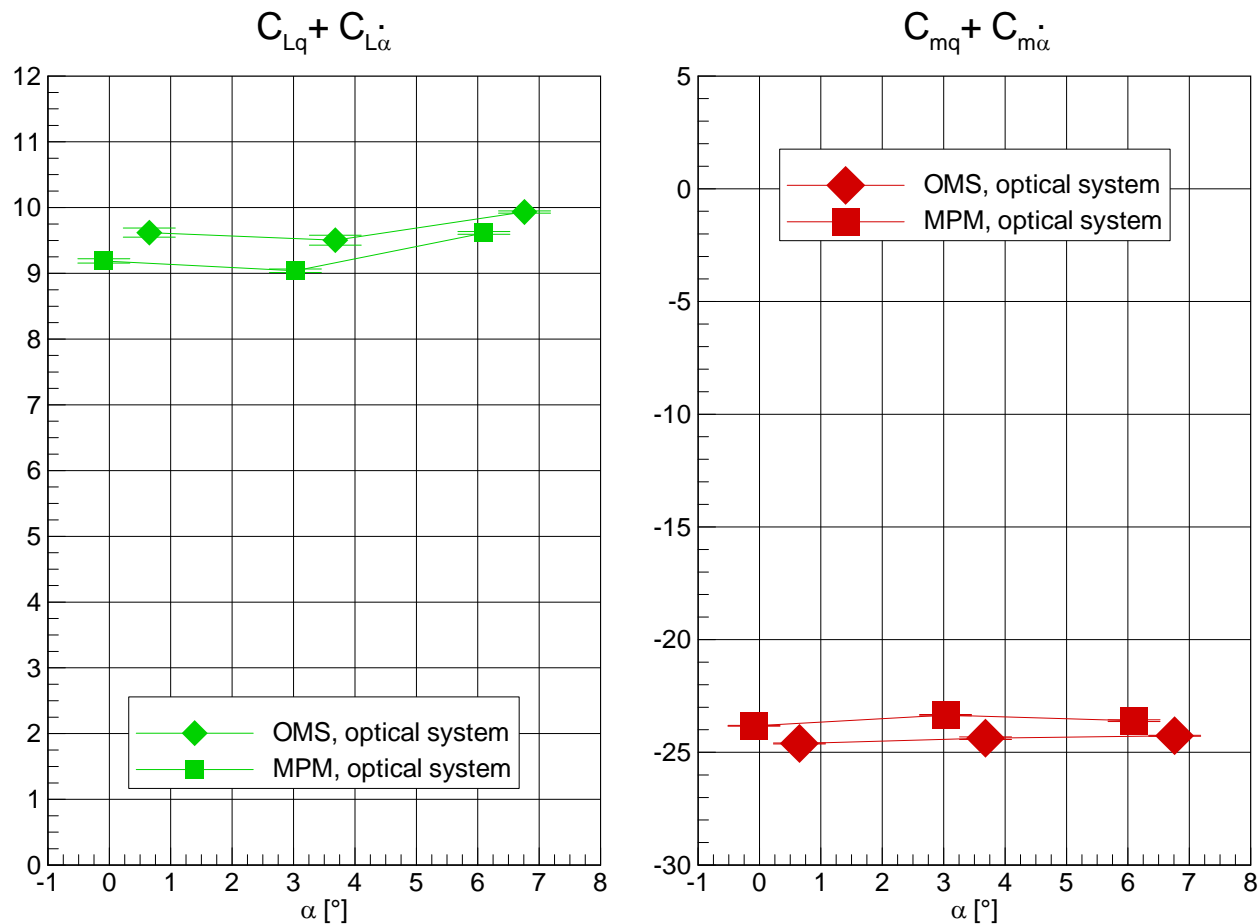
$$C_{l\dot{\beta}}$$

$$C_{n\dot{\beta}}$$

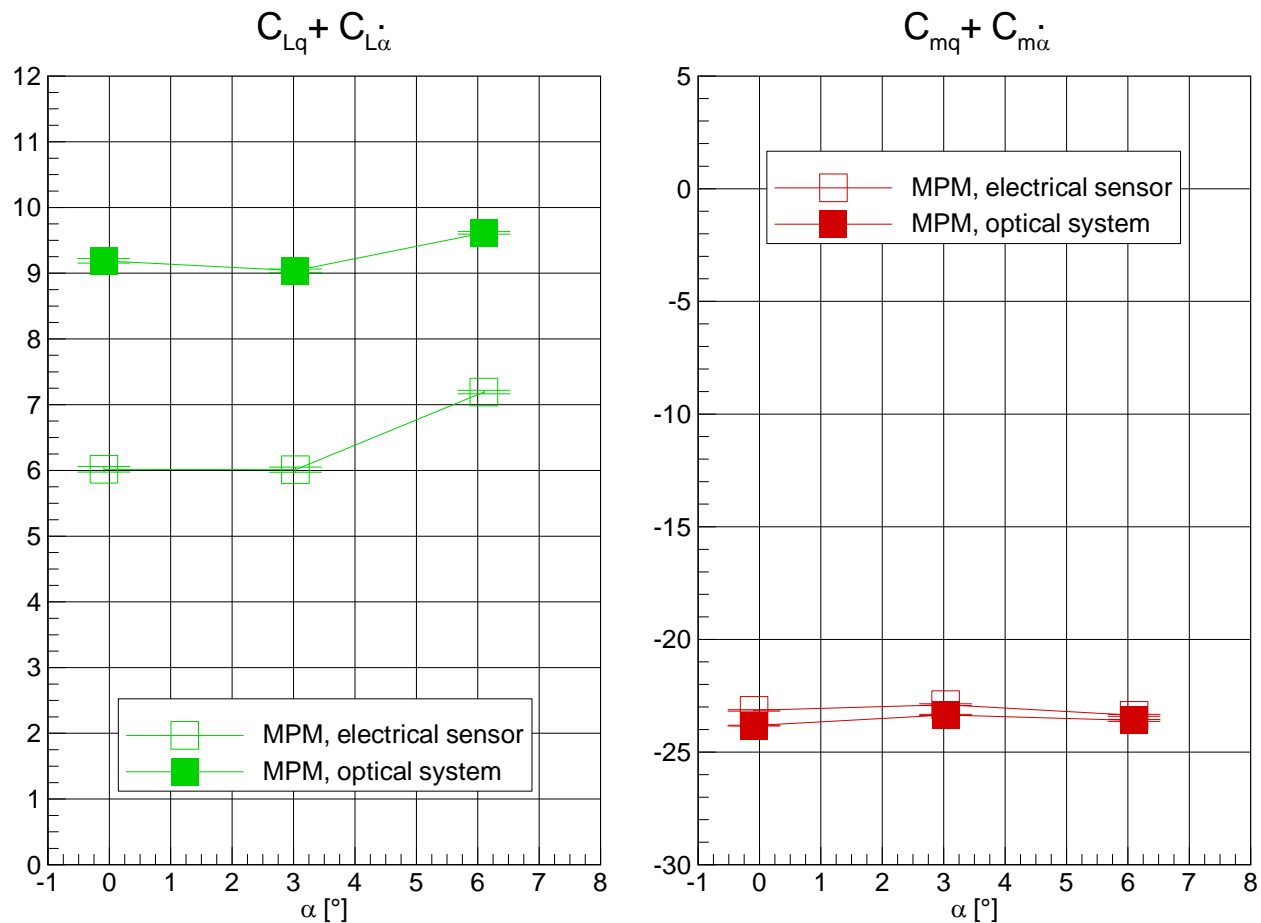
$$C_{Y\dot{\beta}}$$

$$= f(\dot{\beta})$$

Experimental results from OMS and MPM of the DLR-F12 geometry

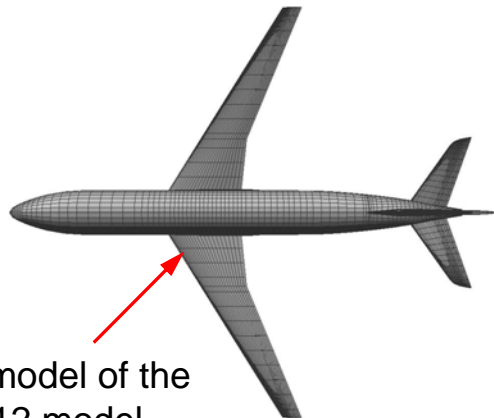


Impact of diff. position measurement techniques on the derivatives of the pitching motion

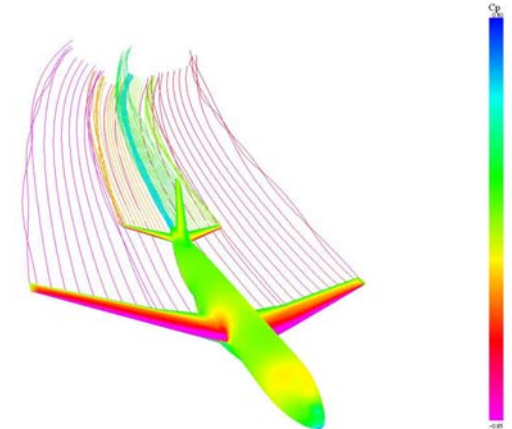


The panel method: VSAERO

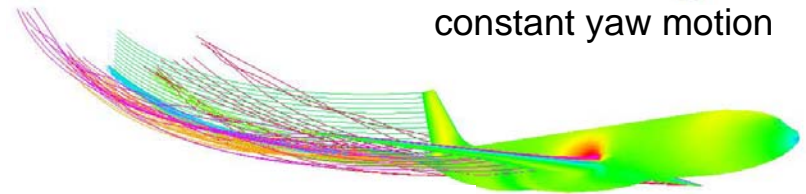
- subsonic panel method for arbitrary body geometry
- wake shape relaxation
- skin friction and boundary layer displacement
- **quasi-steady rotations**



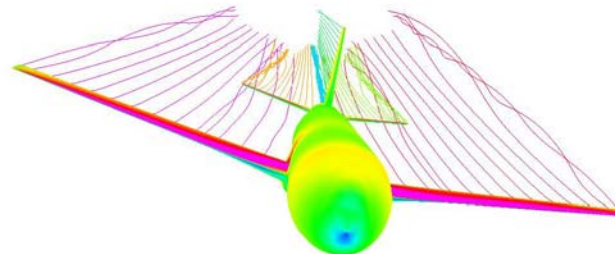
Panel model of the
DLR-F12 model



constant yaw motion

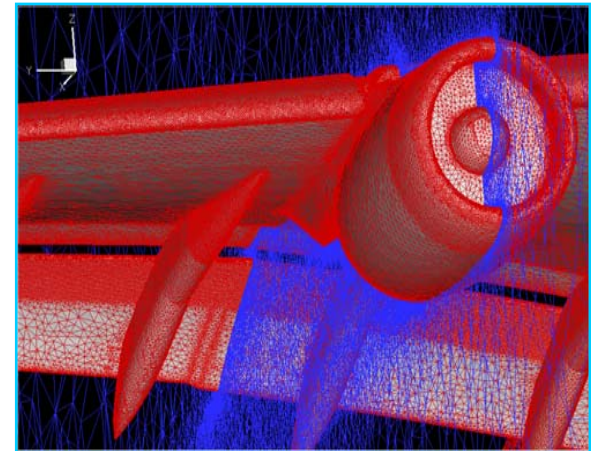
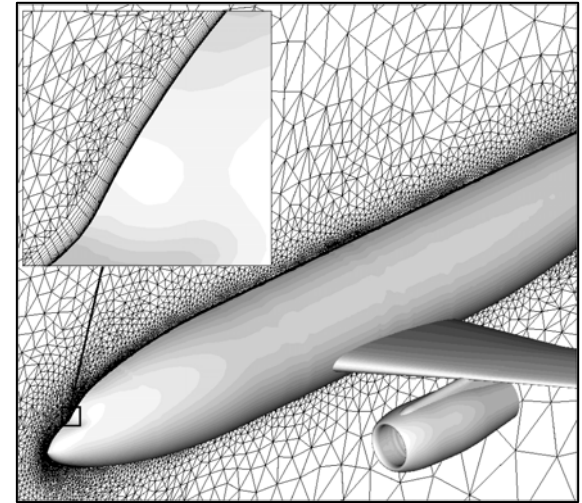


constant pitch motion

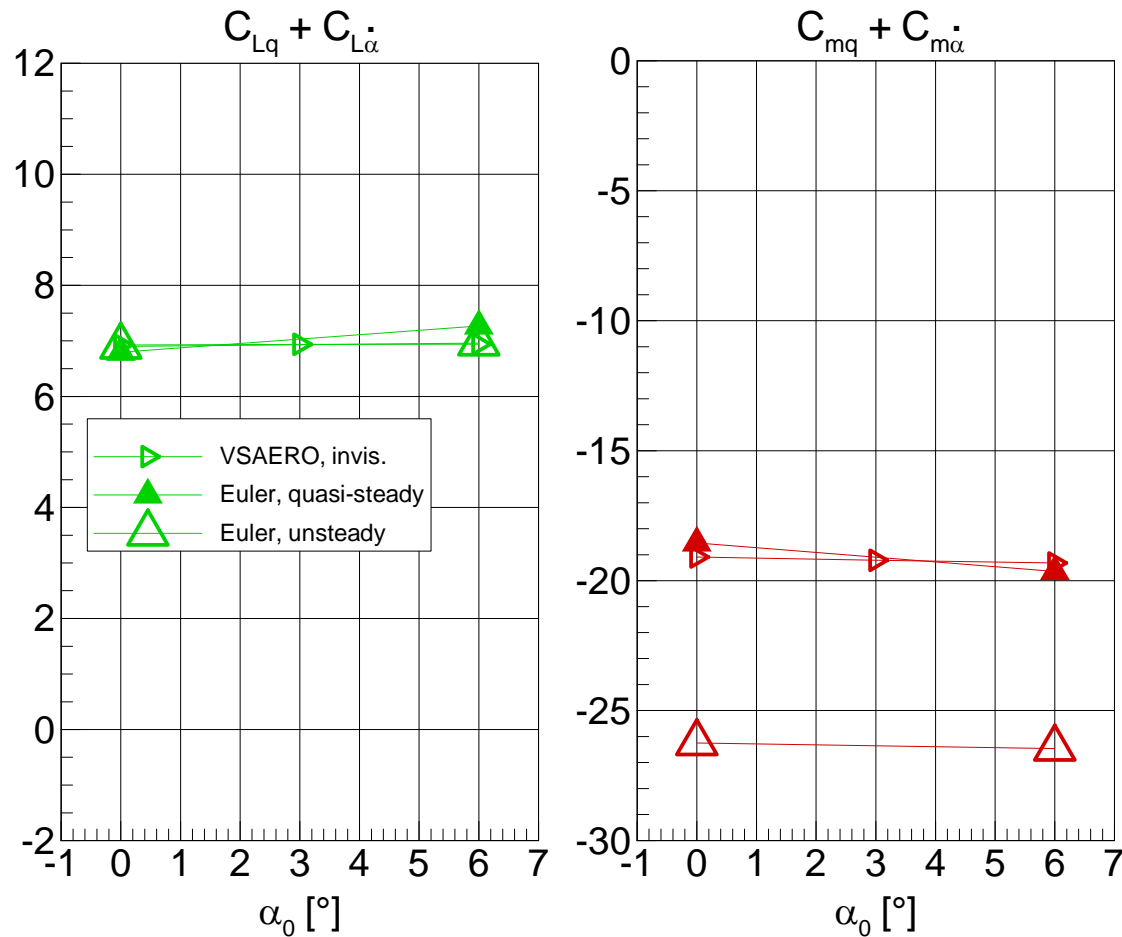


constant roll motion

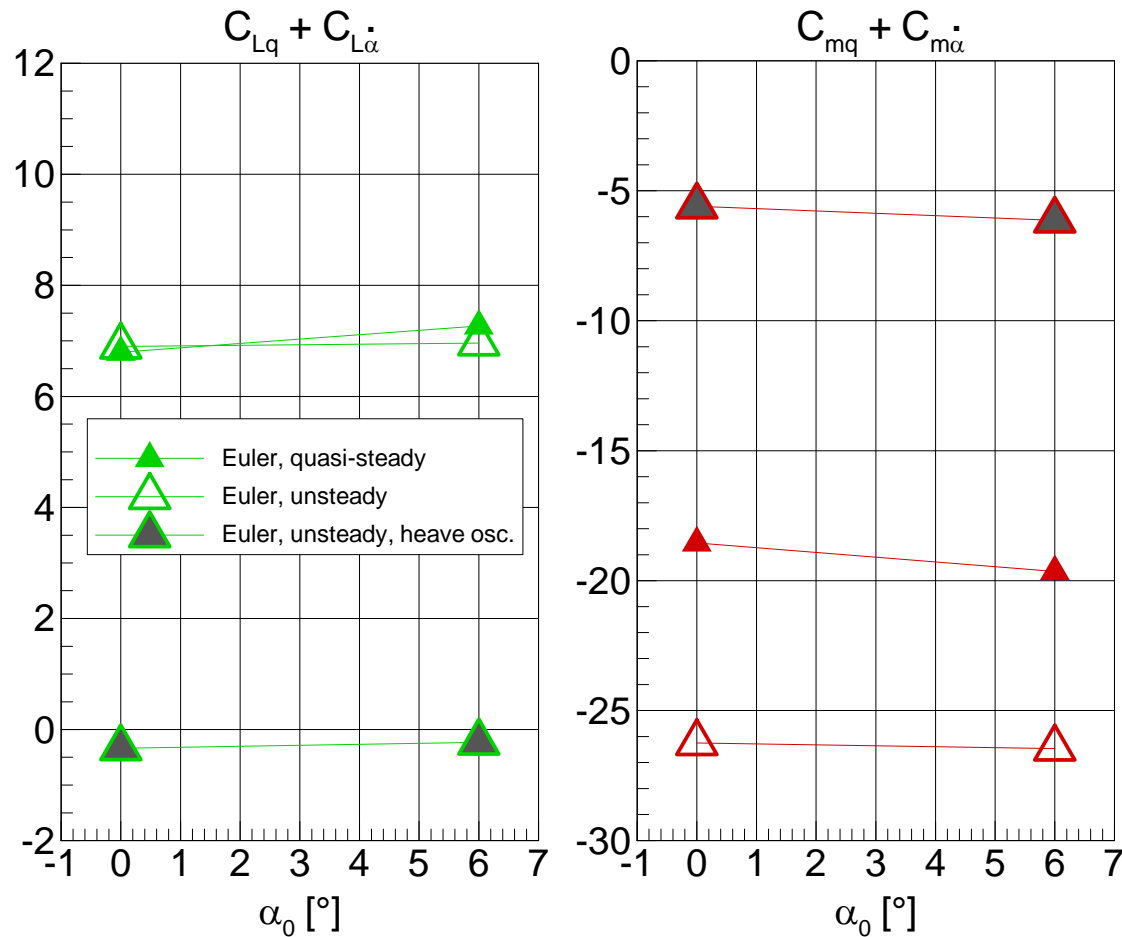
- solution of RANS equations for arbitrary moving bodies on unstructured meshes
- independent of grid cell type (hybrid meshes)
- various turbulence models
- grid adaptation (refinement & de-refinement)
- designed for massively parallel computers
- validated for increasing number of test cases
- routinely used by DLR and Aircraft Industry
- quasi steady / unsteady movements
(steady/unsteady flow)



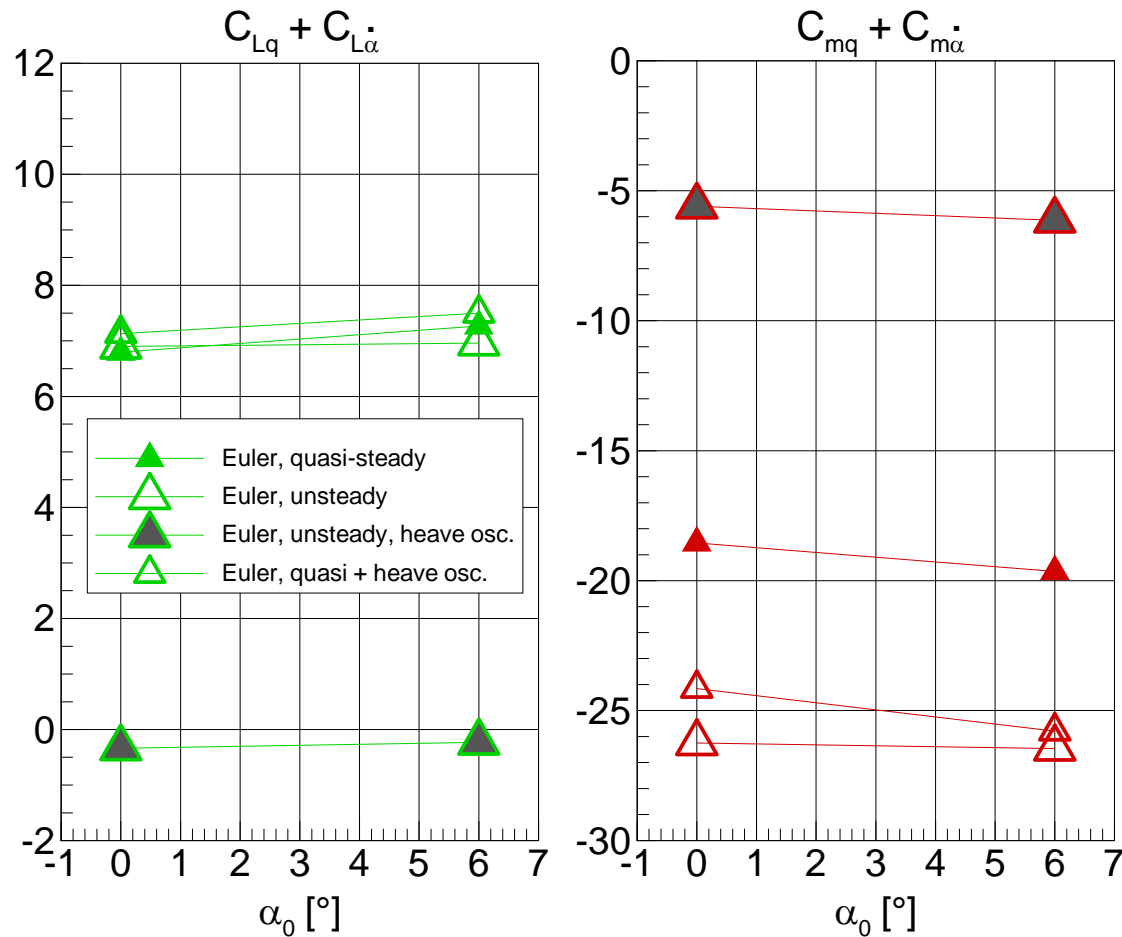
Different shares of derivatives for Euler results, DLR-F12 geometry (1)



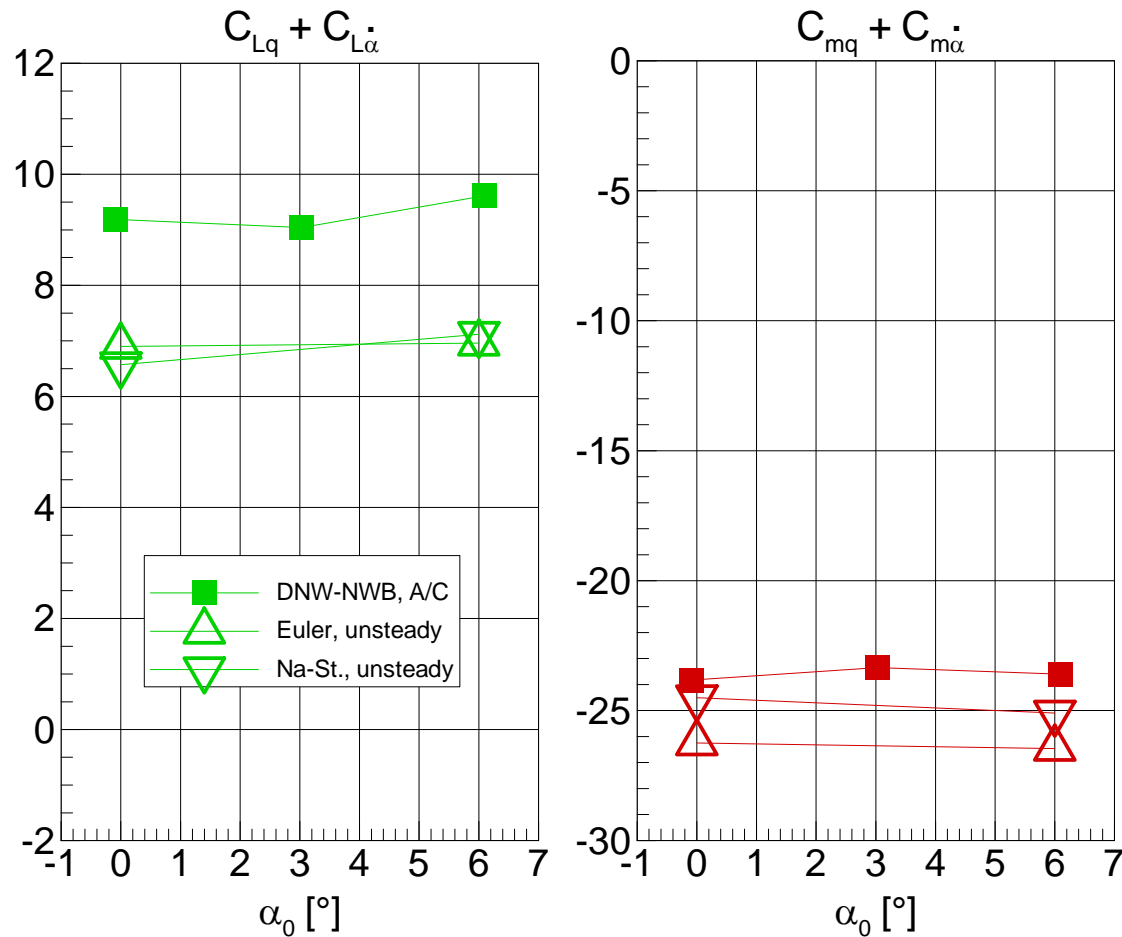
Different shares of derivatives for Euler results, DLR-F12 geometry (2)



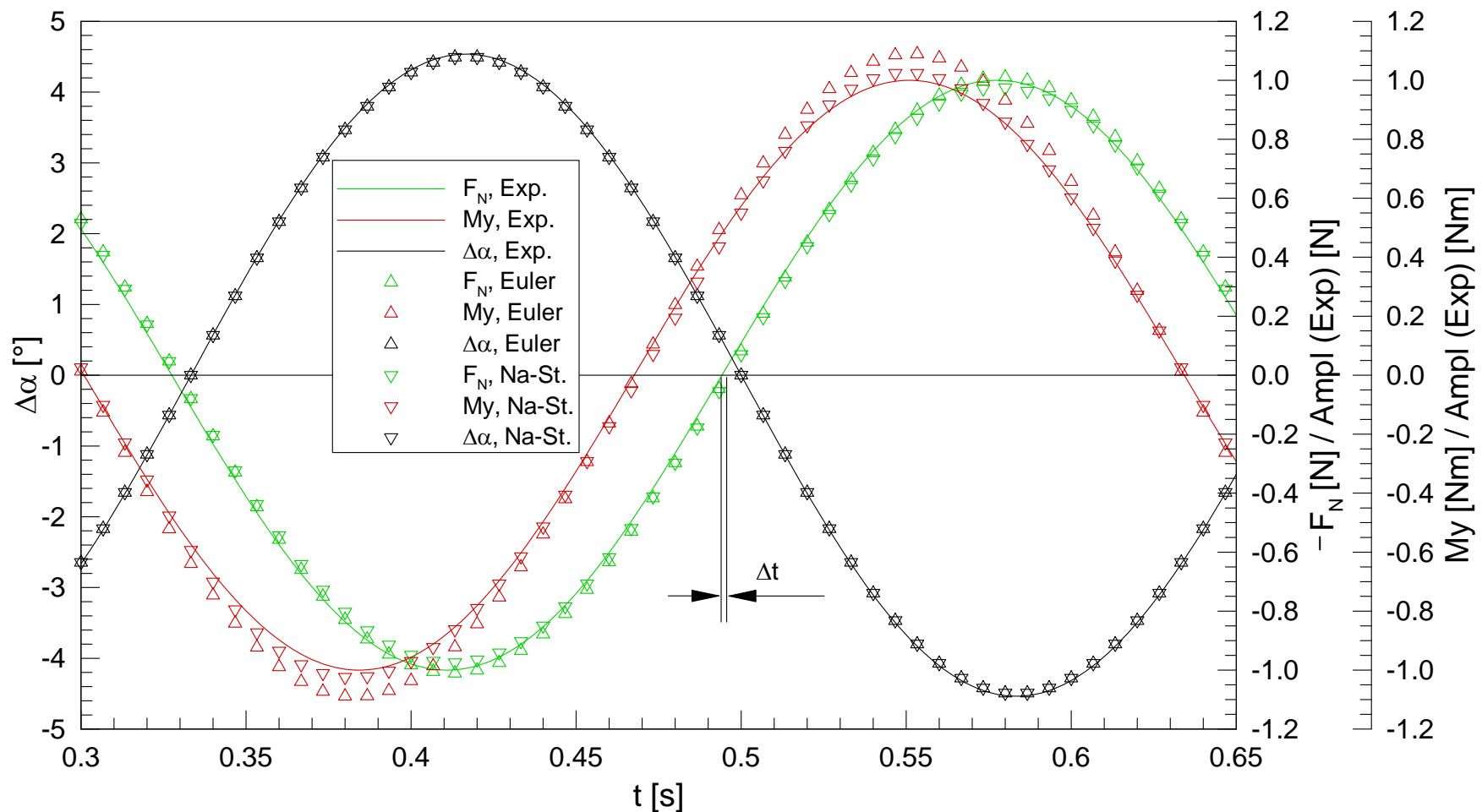
Different shares of derivatives for Euler results, DLR-F12 geometry (3)



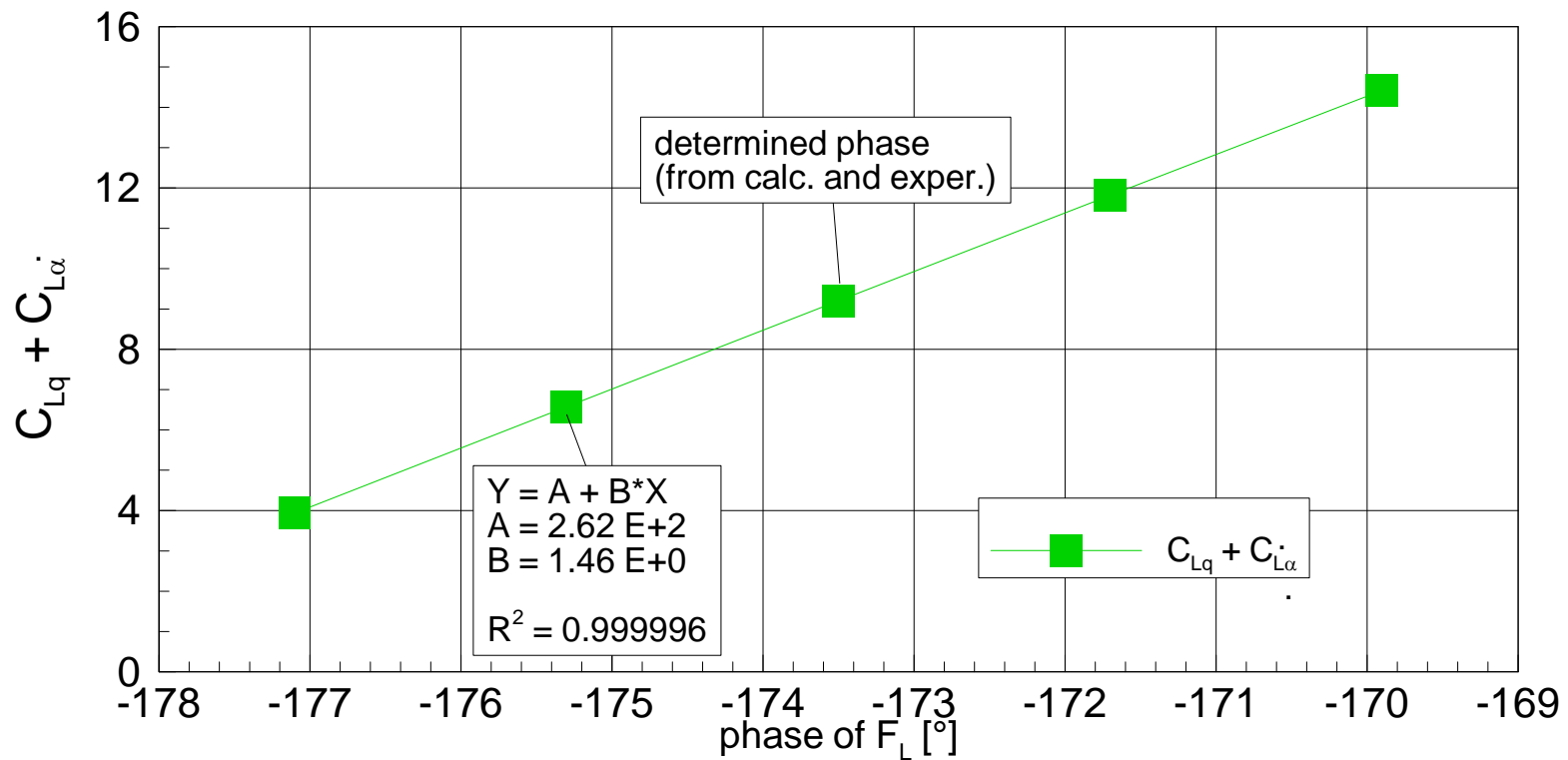
Comparison of numerical and experimental results, DLR-F12 geometry



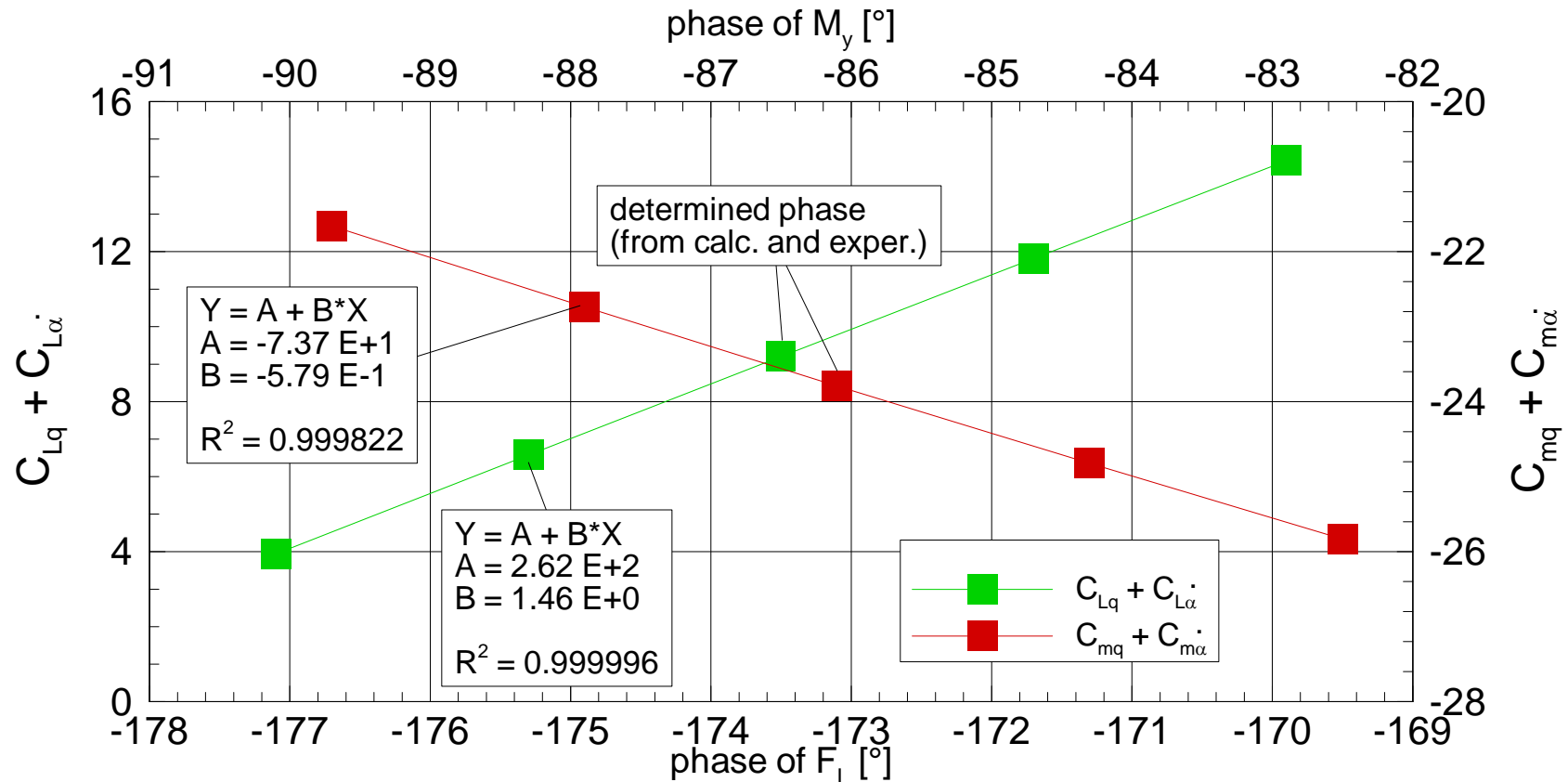
DLR-F12, pitching motion, comparison of experimental and numerical results



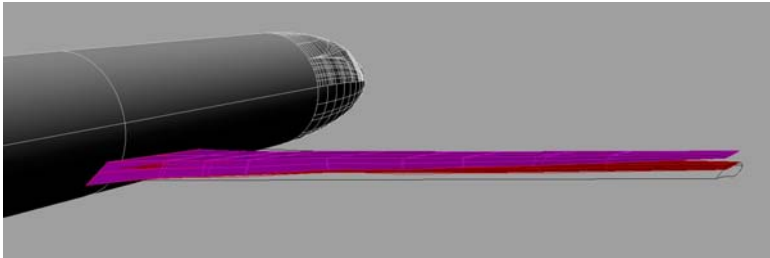
Effects of phase error: Derivative of the pitching oscillation



Effects of phase error: Derivative of the pitching oscillation

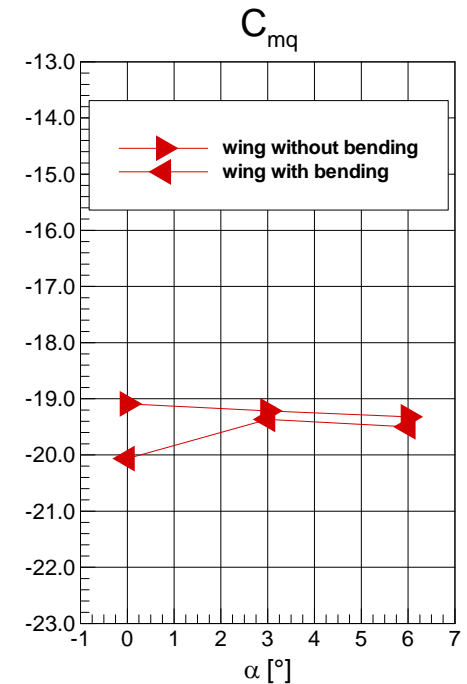
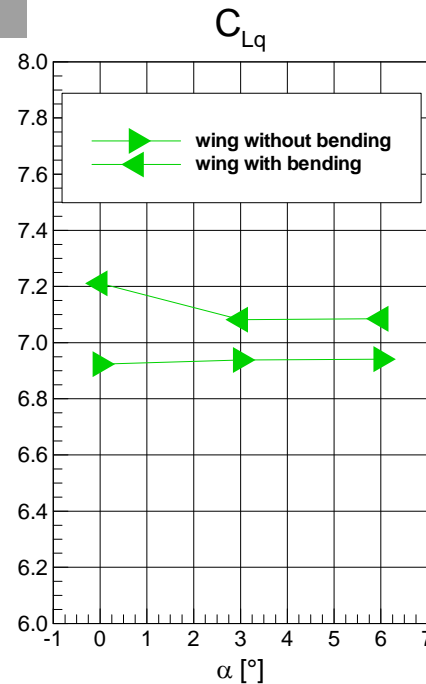


Outlook (1)



Assumption so far:
ideal rigid model without deformation

Very first results from VSAERO
for a rigid bended wing
(quasi steady)



Outlook (2)

- Investigation of a new *elastic* wind tunnel model in 2007
- Determination of the unsteady wing shape during the motion
- Measurements of the unsteady pressure distribution
- Numerical investigations with multidisciplinary codes with coupled aerodynamic-structural solvers